Evaluating Optimal Farm Management of Phosphorus Fertilizer Inputs with Partial Observability of Legacy Soil Stocks*

Chanheung Cho Zachary S. Brown David M. Kling Luke Gatiboni Justin S. Baker

Please **click here** for the latest draft.

October 24, 2024

Abstract

Decades of intensive fertilizer application have led to the accumulation of phosphorus (P) in soils across US cropland. This over-application can have negative consequences for water quality, but a portion of the accumulated P in soils can serve as a substitute for increasingly costly future fertilizer applications. We investigate whether it is economical for farmers to utilize bioavailable legacy soil P stocks (by reducing P fertilizer use) when they are imperfectly observed and soil sampling is costly. Using 5 years of legacy P measurements from maize field trials spanning over a decade in eastern North Carolina, we develop a dynamic programming model of this optimization problem, with farmer decision-making and economic optimization specified as a 'partial-observability Markov decision process' (POMDP). In a novel contribution to the POMDP literature, we analyze how agent preferences over risk and intertemporal substitution affect optimal monitoring and resource use by incorporating an Epstein-Zin preference structure. Using contemporary computational methods for analyzing POMDPs, we find that more risk-averse optimizing agents in the model apply less fertilizer, across a range of bioavailable legacy P stocks. In sensitivity analysis we find that agents are sensitively response to both sustained increases in P fertilizer price (which is a fully observed stochastic state variable in the model) and to decreases in monitoring costs. We discuss the implications of these findings for policy discussions seeking to address environmental externalities of P fertilizer by providing better and cheaper information to farmers about their legacy P soil stocks.

JEL Codes: Q15, Q24, C61, C63
Keywords: Legacy Phosphorus, Risk Preference, State Uncertainty, Epstein-Zin Preference, Partial-Observability Markov Decision Processes

---

*Cho: North Carolina State University (ccho5@ncsu.edu); Brown: North Carolina State University (zsbrown2@ncsu.edu); Kling: Oregon State University (David.Kling@oregonstate.edu); Gatiboni: North Carolina State University (luke_gatiboni@ncsu.edu); Baker: North Carolina State University (jsbaker4@ncsu.edu). The authors thank participants at various conferences and seminars for useful comments and discussions.
Financial Support from the National Science Foundation (NSF) Award #2019435: Science and Technologies for Phosphorus Sustainability.

1 Introduction

Economically efficient management of the agricultural nutrient phosphorus (P) a critical global challenge for ensuring sustainable food production and environmental quality protection. P is imbalanced in the global food system, and some regions lacking sufficient access to synthetic or organic P fertilizers that could boost yields and rural incomes, leaving producers to rely on limited P stocks in nutrient-deficient soils (Zou et al. 2022). In the United States (and in other advanced economies) the main social challenge in P management is the excessive application of P fertilizer on farmlands, which contributes to water quality degradation and eutrophication in surface water systems. In addition, there are concerns that the overuse of P fertilizers in advanced economies depletes mineral stocks and increases prices. However, as illustrated in Figure 1, P fertilizer consumption by US farmers has remained relatively stable over the last few decades and has evidently responded only temporarily to recent and persistent price increases, suggesting relatively price inelastic demand for P in US cropping systems (Denbaly and Vroomen 1993).

Notably, unlike nitrogen fertilizer, P fertilizer application residuals after crop take-up can accumulate in soils. This accumulating soil stock of P – referred to as 'legacy P' – can be stored in non-bioavailable reserves, taken up by future crop plantings, or mobilized by subsequent precipitation events, flowing into water bodies. A significant amount of agricultural land in the US has accumulated legacy P stocks over decades of continuous cultivation application of P from synthetic and organic sources (for example, annually, $>$ 1,000 tonnes of P have been accumulated in the agricultural region of Vermont) (Wironen et al. 2018, Ringeval et al. 2018). Phoshorus runoff into surface water bodies catalyzes eutrophication, which can lead to hypoxic 'dead zones' and greenhouse gas (GHG) emissions (Arrow et al. 2018, Conley et al. 2009, Iho and Laukkanen 2012, Rabotyagov et al. 2014, Paudel and Crago 2020). Downing et al. (2021) estimate a substantial economic cost associated with GHG emissions from eutrophication in freshwater system globally.

Various policies have been proposed to mitigate environmental issues arising from the overuse of P fertilizers, including the Numeric Nutrient Criteria under Clean Water Acts and Binational Phosphorus Reduction Strategy in Lake Erie (US EPA 1995, Lake Erie LaMP 2011), with one notable proposal focusing on incentivizing farmers to substitute legacy, soil-bound P stocks for P fertilizer and to reduce P fertilizer applications (Sattari et al. 2012, USDA 2020). Properly managed,

Figure 1: U.S. Phosphorus consumption and phosphorus fertilizer price

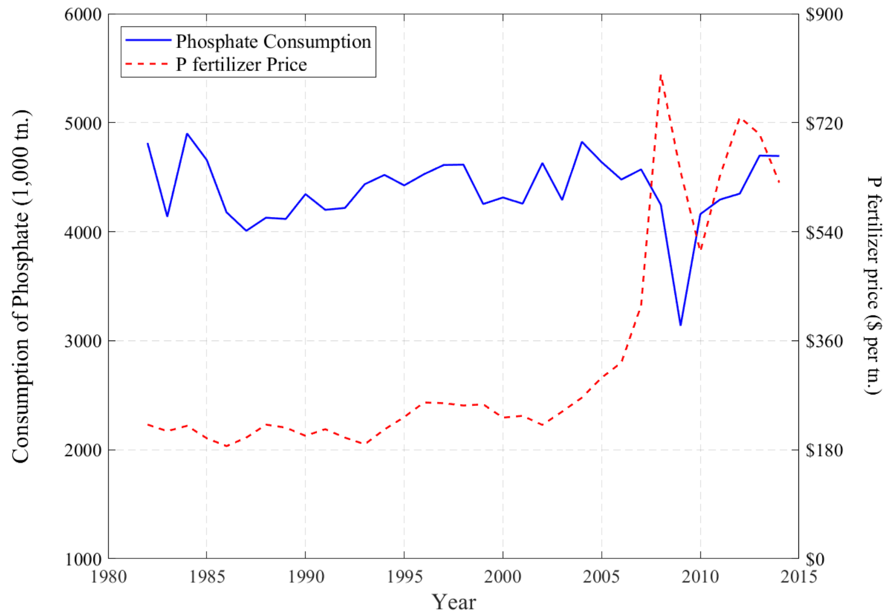

Notes: The graph shows the relationship between P fertilizer consumption and P fertilizer prices from 1982 to 2014. The blue solid line represents P consumption, measured in 1,000 short tons on the left y-axis and the red dashed line indicates the price of P fertilizer, measured in dollars per short ton on the right y-axis.

bioavailable legacy P stocks can substitute for P fertilizer, reducing costs and environmental impacts from intensive crop operations (Sattari et al. 2012). However, this policy idea raises the question of why farmers, in many cases, do not currently utilize legacy P stocks, given their accumulation over time and the potential cost savings for farmers from doing so? This paradox is more pronounced in areas with publicly available information on soil P content provided by state Extension services.

This paper studies this question using a model that incorporates biophysical crop production and legacy P stock dynamics for a representative agricultural system with dynamic farm-scale management incentives and behavioral factors to simulate P stock dynamis in a setting of imperfect information on legacy P bioavailability, market uncertainty, and risk aversion. The complexity of managing legacy P stocks poses significant challenges for farmers and the economic benefits of different strategies recommended by agricultural extension are uncertain. Recent analysis suggests that farmers may not fully account for these residual P stocks in their P fertilizer application decisions due to a lack of high-quality information and the inherent uncertainty about the quantity and bioavailability of legacy P stocks across their farmland. When accounting for farmer risk aversion, the uncertainty surrounding legacy P could contribute to its under-utilization. This paper explores how these factors affect the intertemporal dynamics of legacy P stocks and utilization, and examines whether improved access to enhanced (and higher cost) monitoring of legacy P stocks could reduce P fertilizer application.

To address the management of legacy P accumulated in soil and its losses to surface water, previous studies have analyzed the optimization of fertilizers in farmland along with P control or conservation policies. Schnitkey and Miranda (1993) analyze the optimal steady-state application of fertilizer under various policy settings which limit the soil P level. Goetz and Zilberman (2000) examine the intertemporal and spatial optimal application of mineral fertilizer levels given P concentrations in bodies of water associated with agricultural land for optimal lake restoration policy. Innes (2000) explains that environmental impact of nutrient runoff from livestock production can be mitigated by regulating facility size, implementing waste policies based on cleanup costs, and combining fertilizer taxes with subsidies for manure spreading equipment. Lötjönen et al. (2020) provide a theoretical spatial modeling framework to study climate and water policies for P mineral and manure fertilizer use in dairy farm management. While the models in these studies account for optimal fertilizer usage decisions to manage P accumulation in soils and to reduce P loss to the surface water, they do not incorporate the observational uncertainty related legacy P, and thus cannot answer the question we address here.

Farmers in the US do typically have some baseline information about soil P, as US farmers commonly employ standard soil sampling, provided by state agencies or extension services and by private soil testing service laboratories at nominal fees. These tests can help gauge legacy P availability, among other soil health metrics. Soil tests are usually conducted at a few spots within fields, offering preliminary insight into soil P content, and serving as noisy indicators of the actual bioavailable legacy P stock across a field (Austin et al. 2020). While more comprehensive sampling options exist, offering clearer information on legacy P heterogeneity across a field, they come at a higher cost, presenting a trade-off between accuracy and expense (Austin et al. 2020, Gatiboni et al. 2022).

Economically, this situation can be described as one in which the agent – here, the farmer – optimizes their utilization of an uncertain resource stock – here, legacy P – in which they may dynamically update their beliefs about these fluctuating stocks based on costly monitoring.

Generically, this situation represents a common class of problems in the resource management literature, referred to as a 'partial-observability Markov decision process' or POMDP (Clark 2010, Fackler and Pacifici 2014, Fackler 2014). Previous applications of POMDP models and extensions in resource management have included invasive species control (Haight and Polasky 2010, Rout et al. 2014, Kling et al. 2017), forestry (Sloggy et al. 2020), environmental conservation (White 2005), erosion prevention (Tomberlin and Ish 2007), and infectious diseases (Chadès et al. 2011).

To our knowledge POMDP methods have yet to be applied either in a depletable resource context or in farm production economics (though Sloggy et al.'s forestry application is adjacent to such a setting), reflecting one contribution of this paper. Previous agricultural economics studies have addressed the partial observability and monitoring problem using more heuristic optimization methods that separate inference about unobserved state variables from the optimization. For example, Fan et al. (2020) employ such an approach using state-space models to analyze efficient monitoring of an agricultural pest, but they specifically note the theoretical superiority of a POMDP approach for their application were it not for the computational difficulty of these methods.

Additionally, as far as we are aware, agent risk preferences have not previously been included in POMDP applications, at least in agricultural or resource economics. It is natural to conjecture that risk aversion could strongly affect demand for synthetic alternatives to the uncertain resource, monitoring, and the utilization of uncertain stock resources. Our analysis of that general conjecture represents another contribution. Because standard discounted expected utility in dynamic economic models conflates preference parameters for risk aversion and intertemporal substitution, we employ a widely used recursive utility Epstein-Zin specification to disentangle these effects in our analysis (Epstein and Zin 1991).

We develop our model's empirical foundation through econometric analysis of North Carolina field data on legacy P abundance, stock accumulation, fertilizer application, and yield response in a corn-farming context spanning over a decade. We also account for stochastic crop and P fertilizer price dynamics, which we jointly estimate using publicly available USDA data. This extends the model into what is known as a 'mixed-observability Markov decision process' or MOMDP (Kovacs et al. 2012, Sloggy et al. 2020). Inclusion of these dynamics increases the robustness of our analysis, given that previous studies show that stochastic price dynamics have important effects on other dynamic farm resource management problems, such as crop rotation and cover crop planting

(Livingston et al. 2015, Chen 2022).

Including all the elements described above is a significant computational challenge. In particular, POMDPs involve stochastic dynamic programming in which the agents possess belief states that specify their current subjective probability distributions about imperfectly observed biophysical states, with these beliefs states updated via Bayes' Rule. The specification introduces a high-dimensional state space (i.e. a space of probability distributions) that imposes considerable challenges to numerical computation. To address these challenges, we closely follow recently applied density projection methods (e.g. Zhou et al. 2010, Springborn and Sanchirico 2013, MacLachlan et al. 2017, Kling et al. 2017, Sloggy et al. 2020) that reduce the dimensionality of the belief states, while avoiding some of the restrictions and pitfalls of prior methods (e.g. use of conjugate priors or coarse discretization of the unobserved state). We also use an econometric approach in estimating price dynamics that aids numerical tractability in the MOMDP optimization that is still informed by the empirical analysis: We first econometrically estimate a Markov-switching Vector Autoregressive (MSVAR) model for the price dynamics (supported by statistical tests), and then in the dynamic programming impose a conditional, within-regime equilibrium assumption maintain computational tractability.

We find that optimizing farmers in the model generally employ enhanced soil sampling only at low levels of estimated legacy P stocks. Higher risk aversion generally decreases the reliance on fertilizer application in favor of legacy P stocks. Meanwhile, farmer preferences for profit smoothing over time do not appreciably affect optimal fertilizer use or monitoring. Furthermore, sensitivity analysis with much higher fertilizer prices (e.g. from a sustained global market disruption or a tax on fertilizer) or much lower monitoring costs (e.g. from a subsidy for more intensive soil testing) induce much substitution from fertilizer to legacy P use. These results raise questions about the potential effectiveness of proposed price-based instruments to correct externalities associated with agricultural fertilizer.

This paper's sections proceed as follows. First, a model of legacy P dynamics and crop production is described, capturing both the accumulation and bioavailability of legacy P. Next, the economic and management problems are discussed, outlining how farmers can evaluate the recursive expected utility of their controls, P fertilizer application, and soil sampling in the face of stochastic prices and the unobservable state of legacy P. Then, the methodological framework and specification are presented, including price dynamics and the density projection approach for managing Bayesian belief updating. The application of this model to the corn market provides a practical example of how it can be used to guide decision-making in agriculture. Finally, the results of the model are discussed and are integrated with Epstein-Zin preferences, highlighting the implications of risk preferences in shaping farmers' P fertilizer application and soil sampling decisions.

2 Model Description and Computational Methods

A simplified schematic of our POMDP model is shown in Figure 2, with the biophysical dynamics of legacy P stocks L_t at the top level of the figure. The farmer does not observe L_t but receives signals O_t that depend on past soil sampling s_{t-1}, illustrated in the middle level of the figure. Farm production decisions regarding fertilizer applications F_t and realized profit π_t are also determined at this level. The bottom-level of the figure illustrates farmer inference regarding their unobserved legacy P stocks L_t, with beliefs b_t being updated based on the signal O_t. The following subsections describe the structure and equations for each of these components, as well as the economic optimization problem to be solved.

2.1 A Model of Stochastic Legacy Phosphorus Dynamics

We use a deterministic model of legacy P dynamics from Iho and Laukkanen (2012), to which we add stochastic behavior. The average soil-accumulated legacy P stock per hectare is given by L_t, with its dynamics specified in the following recursive equation:

$$L_{t+1} = \rho_t L_t + (\gamma_1 + \gamma_2 L_t) \underbrace{\left[F_t - \overbrace{(\gamma_3 \log(L_t) + \gamma_4)}^{\text{Concentration on Yield}} Y(L_t, F_t) \right]}_{\text{Legacy P Surplus}} \tag{1}$$

where ρ_t is a 'carry-over' parameter of legacy P, F_t represents the amount of P fertilizer input, and $Y(L_t, F_t)$ is the crop yields at time t. The terms $(\gamma_3 \log(L_t) + \gamma_4)$ defines the legacy P concentration of the crop yield, which increases logarithmically with L_t. As L_t increases, the legacy P concentration also rise, initially leading to augmented yields. However, despite ongoing increases

Figure 2: Schematic of Partially Observable Markov Decision Process

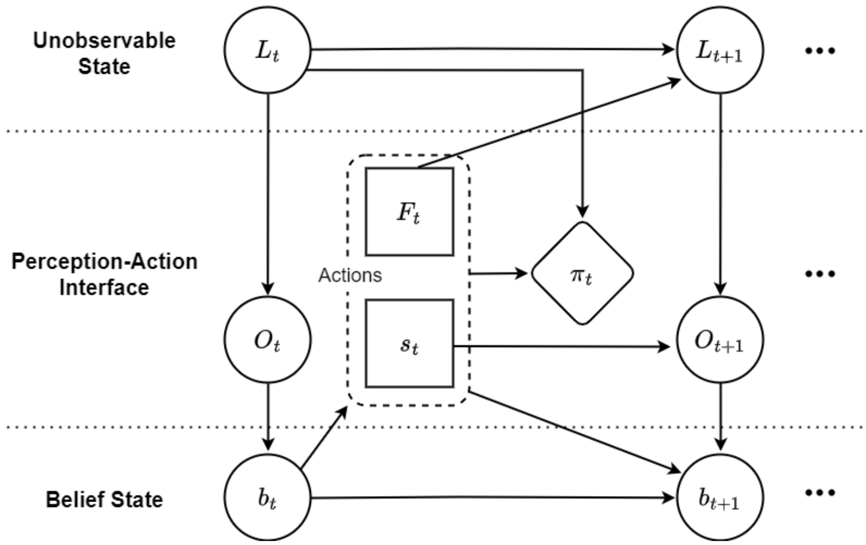

Notes: The farmer infers their unobserved legacy P stock L_t through observations O_t and updates their belief state b_t. Phosphorus fertilizer application F_t and soil sampling s_t influence both the state transition L_{t+1} and future observations O_{t+1}.

in L_t, the marginal yield gains attribute to each additional unit of legacy P progressively diminish. The term $(\gamma_1 + \gamma_2 L_t)$ is explain the change in legacy P brought about by a unit surplus or deficit in legacy P balance (Ekholm et al. 2005). The parameter values of γ are summarized in Table 5.

While there are several empirically-grounded ways to introduce stochastic behavior in this model, we focus on stochastic transport into the environment, owing to precipitation and other environmental factors. In a deterministic model, a carry-over parameter $\rho_t < 1$ implies a decay of soil phosphorus stock on farmland in the absence of further fertilizer inputs, or a loss of soil-bound P to surface water systems (Ekholm et al. 2005, Iho and Laukkanen 2012). We introduce stochasticity into legacy P dynamics by specifying this carry-over parameter as:

$$\rho_t = \exp\left[\left(\mu_\rho - \frac{\sigma_\rho^2(L_t)}{2} + \sigma_\rho(L_t)W_t\right)\right], \qquad \text{with } W_t \sim \mathcal{N}(0,1), \tag{2}$$

where μ_ρ is the log-mean of ρ_t (so that $\mathbb{E}[\rho_t] = \exp \mu_\rho$) and $\sigma_\rho(L_t)$ is the standard deviation of log μ_ρ, with $\sigma_\rho(L_t)$ specified as potentially a function current stocks L_t. We assume $\mu_\rho < 0$, so that the legacy P stock available for crop uptake stochastically decays without added P fertilizer F_t.

Note the log-normal distribution of ρ_t means that a fixed standard deviation σ_ρ would result in the conditional variance of the annual change in legacy P stocks from growing without bound as L_t grows (i.e. $\lim_{L_t \to \infty} \text{Var}(L_{t+1}|L_t) = \infty$), which is not biophysically realistic. Following previous studies that have dealt with similar issues (Loury 1978, Gilbert 1979, Melbourne and Hastings 2008, Sims et al. 2017, Sloggy et al. 2020), we therefore specify the log standard deviation as a decreasing function of the stock. Specifically, in our main specification, we assume that the portion of the stock carried over to the next period ($\rho_t L_t$) has a fixed variance ς^2, invariant with the current stock level L_t. This assumption implies the log standard deviation function takes the form $\sigma_\rho(L_t) = \sqrt{\ln(1 + \varsigma^2 \exp(-2\mu_\rho)/L_t^2)}$. We investigate the importance of this assumption by also considering a fixed log standard deviation ($\sigma_\rho(L_t) = \bar{\sigma}$) in the Appendix.

2.2 Soil Sampling and Partial Observability

Legacy P is not perfectly observed, but farmers in the model receive information through soil sampling. We consider two kinds of soil sampling: standard sampling (ss) and point sampling (ps). Standard sampling, typically provided by state agencies or extension services at nominal fees, involves collecting samples from a few spots within fields. These tests offer preliminary insights into soil P content but serve as noisier indicators of the actual bioavailable legacy P stock across a field (Austin et al. 2020). Point sampling, on the other hand, involves collecting multiple samples at specific grid points or random locations within grid cells, providing more precise information on legacy P bioavailability, but at a higher cost (Austin et al. 2020, Gatiboni et al. 2022).[1]

To specify the observation process, we denote the current soil sample test result as O_t. As a noisy measure of legacy P across the whole hectare of farmland, we assume a multiplicative test error λ which is zero truncated and normally distributed with variance σ_s^2 determined by the type of sampling $s \in \{ss, ps\}$ (Kling et al. 2017).

$$O_t^s = \lambda_t^s L_t, \qquad \text{where } \lambda_t^s \sim \mathcal{TN}(1, \sigma_s^2). \tag{3}$$

The information gained from point v. standard sampling is captured by the assumption that

[1]We exclude the no sampling case in our main analysis because in practice, commercial farmers in the US almost always conduct at least standard sampling, which is offered by state agencies for a nominal fee. This was confirmed in a more elaborate version of the model, which allowed for a no-sampling option: When the sampling cost is negligible, then intuitively the farmer would always acquire the almost-free information.

$\sigma_{ss} > \sigma_{ps}$. In principle, truncation also implies that for a small enough (but positive) level of legacy P relative to the test error variance σ_s^2, the soil test may find zero soil P, which is physically possible though highly uncommon (suggesting generally good test accuracy).

The farmer's beliefs about the distribution of legacy P are denoted by the pdf $b_t(L_t)$, representing a subjective probability distribution over the unobserved L_t, conditional upon the history of controls and resulting observations (Kling et al. 2017). Bayesian updating of these beliefs combines each period's prior beliefs regarding L_t, with projected dynamics for L_{t+1}, along with new information O^s_{t+1}, via the following:

$$b_{t+1}(L_{t+1}) \propto p(O^s_{t+1} \mid L_{t+1}, s_t) \int p(L_{t+1} \mid L_t, F_t) b_t(L_t) dL_t \tag{4}$$

with a given $b_0(L_0)$ specifying the prior beliefs about initial stocks and where $p(O^s_{t+1}|L_{t+1}, s_t)$ is the conditional pdf of the observation. The Markovian properties ensure that the next period beliefs only depend on the current beliefs, controls, and information gained in the current period. Figure 2 illustrates how the farmer updates their belief state b_t based on their soil sampling decision s_t and resulting soil test result O^s_t.[2]

2.3 Economics and Management

Annual payoffs in the model are evaluated as the profit determined by crop yields and stochastic prices. Formally, the expected (partial) profit is specified as the per hectare production function $Y(L_t, F_t)$ and stochastic prices:

$$\pi(L_t, F_t, P^Y_{t+1}, P^F_t, s_t) = P^Y_{t+1} Y_t(L_t, F_t) - P^F_t F_t - c_s s_t, \tag{5}$$

where P^Y_{t+1} and P^F_t are prices for the crop and P fertilizer, respectively, and c_s is a soil sampling cost (with $c_{ss} < c_{ps}$), and $s_t \in \{ss, ps\}$ reflects the soil sampling decision at time t. Fertilizer application decisions are based on the observed fertilizer price P^F_t at the time of application, whereas the

[2] In principle, in addition to soil test results, farmers could infer the adequacy of their soil P stocks through observed yields (e.g. by observing yields when no fertilizer is applied). Modeling belief-updating with this additional information source is significantly more complicated. However, we did undertake this effort, the results of which - shown in the Appendix - suggest that at least in our application such a yield signal provides very little information relative to soil tests. We thus exclude this additional complication from the main model and results presented here.

crop price P^Y_{t+1} will only be realized at the end of the season and not yet observed at the time of applying fertilizer. This means that the decision to apply fertilizer is informed by the current fertilizer price and the last harvest's crop price. Dynamics for the prices $\boldsymbol{P}_t = [P^Y_t, P^F_t]$ are assumed to be determined by a joint Markov process, such that $\boldsymbol{P}_{t+1} = G(\boldsymbol{P}_t, \boldsymbol{\epsilon}_t)$ where $G(\cdot)$ is a transition function and $\boldsymbol{\epsilon}_t$ is a vector of price shocks driven by macroeconomic conditions or short-term exogenous shocks. We discuss the specific structure used for these dynamics below in econometric estimation for our application.

A risk-neutral farmer agent with no preference for profit-smoothing over time and a fixed discount rate would seek to maximize the expected net present value (ENPV) of their profits. For an agent with an infinite time horizon (or a stochastic time horizon with a constant hazard rate of termination), the Bellman equation characterizes the maximal ENPV as a function $V(\boldsymbol{S}_t)$ of the observed state variables collected in $\boldsymbol{S}_t \equiv [b_t(\cdot), P^Y_t, P^F_t]$, and can be written as follows:

$$V(\boldsymbol{S}_t) = \max_{F,s} \ \Pi(\boldsymbol{S}_t, F_t, s_t) + \beta \mathbb{E}\big\{V(\boldsymbol{S}_{t+1}) \mid \boldsymbol{S}_t, F_t, s_t\big\}, \tag{6}$$

where β is the discount factor and $\Pi(\boldsymbol{S}_t, F_t, s_t)$ are expected end-of-season profits given currently observed states and actions:

$$\Pi(\boldsymbol{S}_t, F_t, s_t) \equiv \iint \pi(L_t, F_t, P^Y_{t+1}, P^F_t, s_t) f(P^Y_{t+1} \mid P^Y_t, P^F_t) b_t(L_t) dP^Y_{t+1} dL_t \tag{7}$$

where $f(P^Y_{t+1}|P^Y_t, P^F_t)$ is conditional pdf of crop price P^Y_{t+1} at the upcoming harvest, given the last observed harvest price P^Y_t and current fertilizer price P^F_t.

In this paper, we are interested in studying how risk and intertemporal preferences affect optimal monitoring of the unobserved state of legacy P, L_t. To do so, we generalize the above Bellman equation via the commonly used Epstein-Zin recursive preference structure. Originally developed in the macro-finance literature to allow nontrivial risk premiums in empirically-defensible capital asset pricing models (Epstein and Zin 1989), this preference structure has since been applied in dynamic agricultural production-inventory models (e.g. Lybbert and McPeak 2012), valuation of ecological insurance (Augeraud-Véron et al. 2019), and in integrated assessment models for evaluating the economic damages from climate change (Cai and Lontzek 2019). The key advantage of Epstein-Zin preferences is that they disentangle risk aversion from preferences for intertemporal smoothing, which are conflated in expected discounted utility models. For our purposes, this allows us isolate how risk aversion versus intertemporal smoothing preferences affect optimizing agents' demand for monitoring.

The Bellman equation for the recursive expected utility function, given Epstein-Zin preferences, is as follows:

$$V_{EZ}(\boldsymbol{S}_t) = \max_{F,s} \left[(1-\beta)\Pi_{EZ}(\boldsymbol{S}_t, F_t, s_t)^{1-\psi^{-1}} + \beta\mathbb{E}\left\{V_{EZ}(\boldsymbol{S}_{t+1})^{1-\eta} \mid \boldsymbol{S}_t, F_t, s_t\right\}^{\frac{1-\psi^{-1}}{1-\eta}}\right]^{\frac{1}{1-\psi^{-1}}}, \tag{8}$$

where $\Pi_{EZ}(\boldsymbol{S}_t, F_t, s_t)$ is the certainty-equivalent expected utility of end-of-season profits:

$$\Pi_{EZ}(\boldsymbol{S}_t, F_t, s_t) \equiv \left(\iint \pi(L_t, F_t, P^Y_{t+1}, P^F_t, s_t)^{1-\eta} f(P^Y_{t+1} \mid P^Y_t, P^F_t) b_t(L_t) dP^Y_{t+1} dL_t\right)^{\frac{1}{1-\eta}} \tag{9}$$

and where η and ψ indicate, respectively, the coefficient of relative risk aversion (RA) and the elasticity of intertemporal substitution (EIS): Higher η and ψ correspond respectively to greater risk aversion and a weaker preference for intertemporal smoothing, with $\eta = \psi^{-1}$ reducing EZ preferences to the expected discounted utility preference structure and $\eta = \psi^{-1} = 0$ ($\psi = \infty$) reducing the EZ Bellman equation to Bellman eq. (6) for the risk neutral agent with perfectly elastic intertemporal substitution.[3]

2.4 Computational Methods: Density Projection and Particle Filtering

Note that one of the state variables in the above dynamic program is the continuous belief pdf $b_t(\cdot)$, which makes the model computationally intractable in its current form. Various methods have been proposed to address this common problem in POMDPs and related adaptive management applications, the simplest of which is to specify an initial prior belief pdf $b_0(\cdot)$ that is conjugate to likelihood function, so that $b_1(\cdot)$, $b_2(\cdot)$ and so for $b_t(\cdot)$ remain in the same family (e.g. normal distribution). This reduces the belief state from an infinite dimensional continuous pdf to a low-dimensional belief state corresponding to the parameters of that family (e.g. mean and variance of normal distribution). However, the use of conjugate priors is overly restrictive for most modern

[3]In this case, the value function in the EZ Bellman equation, $V_{EZ}(\boldsymbol{S})$ is simply a rescaling of the risk neutral value function by $V_{EZ}(\boldsymbol{S}) = (1-\beta)V(\boldsymbol{S})$.

resource management problems, particularly in POMDP applications where the dynamics of the unobserved state variable L_t need to be accounted for in belief updating, via the pdf $p(L_{t+1} \mid L_t, F_t)$ representing the stochastic transition dynamics.

To address this challenge, we follow the prevailing alternative in the resource economics literature involving density projection and particle filtering. The full algorithm used here is the same one employed by Kling et al. (2017) and Sloggy et al. (2020) in other resource management applications, and for completeness is detailed in the Appendix. In summary, the method first specifies a parametric distribution family for prior beliefs $b_t(L_t)$- here, a log-normal distribution, parameterized by a measure of central tendency and uncertainty: We parameterize the log-normal pdf here by its arithmetic mean μ^L and coefficient of variation ν^L. The method then takes the pdfs for these prior beliefs, the conditional likelihood of the observations $p(O^s_{t+1} \mid L_{t+1}, s_t)$, and the transition dynamics $p(L_{t+1} \mid L_t, F_t)$, and uses particle filtering with Bayes' rule in eq. (4) to simulate draws from the posterior updated beliefs $b_{t+1}(L_{t+1})$. This posterior belief pdf is no longer log-normal; however, density projection is used to fit an approximating log-normal distribution to the posterior draws, by minimizing a measure of distance between the approximating pdf and the true posterior captured in the draws from the particle filter. Density projection uses the Kullback-Liebler divergence as the distance measure between the approximating and prior pdfs. This results in the approximating distribution's distance-minimizing parameters effectively being maximum-likelihood estimates, treating the particle filter draws as observations. This procedure ensures that belief-updating only requires updating the mean and coefficient of variation.

This density projection projection procedure is integrated into computation of the dynamic programming solutions, by first discretizing the belief state parameters and actions $(\mu^L_t, \nu^L_t, F_t, s_t)$ and then calculating the discretized transition probabilities for the next-period belief parameters $(\mu^L_{t+1}, \nu^L_{t+1})$. These transition probabilities are pre-computed, before solving the infinite-horizon Bellman equation using standard value- or policy-iteration algorithms for discrete-state dynamic programming (see Appendix).

Table 1: Summary Statistics of North Carolina Tidewater Data

Variable	Obs	Mean	Median	IQR	SD	Min	Max
Legacy P (mg/dm^3)	139	63.986	46	37–66.75	50	28	279
P application (kg/ha)	139	47.036	22	11–67	53.948	0	168
Corn yield (kg/ha)	139	4751.9	4442	2266.7–6517.9	2950.3	131	13712

Notes: Interquartile Range (IQR) is a measure of statistical dispersion, being equal to the difference between the 75th and 25th percentiles. It represents the range within which the central 50% of the data lie.

3 Application to Eastern North Carolina Corn Farming and Econometric Estimation

We apply the model in the previous section to a representative corn production system in eastern North Carolina. This illustrative case study represents This section describes the econometric estimation of model parameters for this context. The first subsection describes estimation of the yield function, and the second describes the joint estimation of US corn and P fertilizer price dynamics.

3.1 Production function estimation and model parameterization

Estimation of the yield function here uses field trial data from the eastern North Carolina Tidewater region described by (Morales et al. 2023), which contains measurements of yields, (experimentally controlled) P fertilizer inputs, and legacy P.

Table 1 provides the summary statistics and evidence of the presence of outliers in the data. For example, in the Legacy P (mg/dm^3), the mean value is 63.986 mg/dm^3, while the median is 46 mg/dm^3. This large difference between the mean and median suggests the presence of high legacy P values that are pulling the mean upwards, indicating potential outliers. Additionally, the maximum value for legacy P is 279 mg/dm^3, which is significantly larger than the interquartile range (IQR) of 37 to 66.75 mg/dm^3, further highlighting the presence of extreme values in the dataset. Similar patterns can be observed in the P fertilizer application and corn yield variables, where the maximum values (168 kg/ha and 13,712 kg/ha, respectively) are far greater than the IQR ranges, reinforcing the conclusion that the dataset contains outliers. These outliers can influence the results of traditional mean based methods, justifying the use of median regression to better capture the central tendency and heterogeneity of the data without being overly influenced by extreme values and so we apply median regression modeled as:

$$\ln(Y_{i,t}(L_{i,t}, F_{i,t})) = \beta_0 + \beta_1 \ln(F_{i,t}) + \beta_2 \ln(L_{i,t}) + \beta_3 \ln(F_{i,t})^2 + \beta_4 \ln(F_{i,t}) \ln(L_{i,t}) + \omega_i + \epsilon_{i,t}, \quad (10)$$

where i denotes experiment plot, ω_i is the experimental replication fixed effect, and $\epsilon^Y_{i,t}$ is a time-varying error component. The experimental replication refers to the distinct replications of the experiment conducted under controlled but potentially varying conditions across different locations. Each replication captures the same treatment levels (e.g., P fertilizer inputs), but the replications themselves may experience variations due to unobserved factors such as subtle differences in soil properties, localized weather conditions, or small operational differences in how the experiments were executed. These replications help ensure that the results are not influenced by one-off conditions specific to a single trial, providing a broader understanding of the treatment effects.

Given that each replication may have its own unique, unobserved characteristics, we include fixed effects for experimental replication. These fixed effects allow us to control for any unobserved, time-invariant factors specific to each replication that could bias the results if not accounted for. By introducing replication-level fixed effects, we can isolate the true impact of the key variables on corn yield, while filtering out the effects of within-replication variability.

To estimate the parameters in the yield response function, we analyze data covering 5 years of field experiments (2010, 2012, 2014, 2021, and 2022) at the North Carolina Cooperative Extension Tidewater Research Station on the coastal plain. These experiments measured legacy P bioavailability measured by Mehlich 3 method and reported in milligrams per cubic centimeter of soil (mg/dm^3), P fertilizer application (kg/ha), and corn yield (kg/ha).

The results in Table 2 estimate the relationship between corn yield and P fertilizer application ($F_{i,t}$) and legacy P ($L_{i,t}$), using a quadratic specification. The positive sign for $\ln(F_{i,t})$ indicates that increasing P fertilizer leads to higher corn yields, suggesting that more fertilizer boosts productivity. However, the negative sign for the quadratic term $\ln(F_{i,t})^2$ implies diminishing marginal returns to P fertilizer application. This means that as more fertilizer is applied, the incremental yield gains begin to decline, reflecting the principle of diminishing marginal productivity commonly seen in agricultural inputs.

Table 2: Corn yield estimation

Log Corn Yield (kg/ha)	
$\ln(F_{i,t})$	0.891**
	(0.415)
$\ln(L_{i,t})$	0.680
	(0.696)
$\ln(F_{i,t})^2$	-0.0125
	(0.0349)
$\ln(F_{i,t}) \times \ln(L_{i,t})$	-0.158
	(0.154)
Constant	4.891**
	(2.401)
Experiment Fixed Effect	Yes
Observations	139
Adjusted R-squared	0.419

Notes: Experiment plot clustered standard errors in parentheses. The standard errors are adjusted for clustering in soil sampling plots. *, **, and *** denote significance at the 10%, 5%, and 1% levels, respectively.

For legacy P ($\ln(L_{i,t})$), the positive sign suggests that higher levels of legacy P could increase yields, although this effect is not statistically significant. The interaction term between $F_{i,t}$ and $L_{i,t}$ has a negative sign, indicating that when both P fertilizer and legacy P are present at high levels, they may act as substitutes, reducing each other's effectiveness. This could imply that as legacy P increases, the marginal benefit of applying additional P fertilizer decreases, which is consistent with the concept of nutrient saturation.

3.2 Corn and phosphorus fertilizer prices

To estimate a dynamic model for corn and fertilizer prices, we analyze USDA time series on corn and P fertilizer prices from 1982 through 2013 (Figure 3). We use P fertilizer (44%-46% phosphate) price data from the USDA "Fertilizer Use and Price" report and corn price data from the

Figure 3: Inflation-adjusted corn and phosphorus fertilizer prices

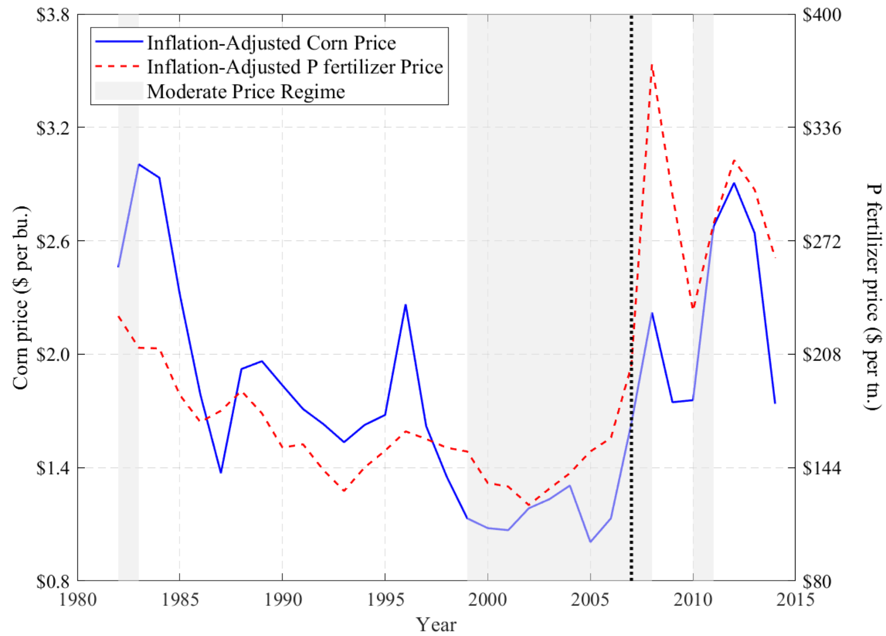

Notes: Inflation-adjusted prices are adjusted using the Consumer Price Index (CPI) for all urban consumer (index 1983=100), with data sourced from the Federal Reserve Bank of Minneapolis (2024.04). The vertical line marks 2007, where dynamics appear to qualitatively change. The Moderate Price Regime, shown in gray, was estimated based on the Markov-switching Vector Autoregressive model.

USDA's "U.S. Bioenergy Table" (USDA 2024a, USDA 2024b), spanning 33-years (1982-2014). For both empirical reasons and to facilitate MOMDP numerical implementation, we estimate price dynamics using a MSVAR model. Markov-switching method generalizes the standard multivariate time-series vector autoregression model by allowing for probabilistic regime transitions in the regression intercepts and coefficients, in order to accommodate qualitative changes observed in the nature of the price dynamics (Hamilton 1989). In our application, use of MSVAR is empirically motivated by observing abrupt and sustained change in corn and P fertilizer price patterns after ca. 2007, as seen in Fig. 3. Before 2007, the inflation-adjusted prices of both corn and P fertilizer show a clear decreasing trend, whereas after 2007 corn and P fertilizer prices beginning to rise significantly. This rise aligns with the global increase in commodity prices more broadly, consistent with a discrete change in market dynamics.

We thus estimate a log-linear MSVAR specification of of the following form:

$$\ln \boldsymbol{P_{t+1}} = \boldsymbol{\mu}_{(r_{t+1})} + \boldsymbol{\Phi}_{(r_{t+1})} \ln \boldsymbol{P}_t + \boldsymbol{\epsilon}_{t+1}, \quad \text{where} \quad \epsilon_{t+1} \sim \mathcal{N}(0, \boldsymbol{\Sigma}), \tag{11}$$

Table 3: Markov-switching vector autoregressive model for corn and phosphorus fertilizer prices

	Corn ($\ln(P^Y_{t+1})$)		Phosphorus fertilizer ($\ln(P^F_{t+1})$)	
	Moderate	High	Moderate	High
$\ln(P^F_t)$	0.105***	0.096***	0.472***	0.469***
	(0.009)	(0.009)	(0.011)	(0.010)
$\ln(P^Y_t)$	0.344***	0.346***	-0.013	-0.008
	(0.010)	(0.010)	(0.009)	(0.009)
$\mu_{(S_t)}$	0.748***	1.274***	0.834***	1.321***
	(0.053)	(0.051)	(0.053)	(0.052)
Variance (Σ_{11})	0.072	Variance (Σ_{22})	0.059	
	(0.0002)		(0.0002)	
Covariance	0.0165			
($\Sigma_{12} = \Sigma_{21}$)	(0.0001)			

Notes: Standard errors are in parentheses. In the estimation, constant variance of residual $\boldsymbol{\Sigma} = \boldsymbol{\Sigma}_{(i)} = \boldsymbol{\Sigma}_{(j)}$ is assumed for $r_t \in \{i, j\}$, $i \neq j$. *, **, and *** denote significance at the 10%, 5%, and 1% levels, respectively.

where $\ln \boldsymbol{P_{t+1}}$ is the vector of corn and P fertilizer prices, $\ln \boldsymbol{P_{t+1}} \in \mathbb{R}^2$ and $\boldsymbol{\Phi}_{(r_{t+1})}$ represents the autoregressive coefficient that vary depending on the regime r_{t+1}. $\boldsymbol{\mu}_{(r_{t+1})}$ is the regime-specific intercept, $\boldsymbol{\Sigma}$ is the covariance matrix of the error terms. In addition, the probability of regime r_{t+1} can be specified as $p_{ij} = \Pr(r_{t+1} = i \mid r_t = j)$ where p_{ij} represents the probability of transition from regime j at time t to regime i at time $t+1$ (Hamilton 1989). We allow for two price regimes in the model, $r_t \in \{\text{moderate, high}\}$, based on visual inspection of the data.

To estimate the MSVAR, we employ a Bayesian approach used by Osmundsen et al. (2021) to estimate the transition probability of the MSVAR model with two regimes, moderate and high. In this model, the system can transition between two distinct regimes, each characterized by different autoregressive coefficient and covariance structures. We estimate the coefficients of the MSVAR model using a Hamiltonian Monte Carlo (HMC) method implemented via the Stan software (Osmundsen et al. 2021). Unlike traditional Gibbs sampling, HMC leverages gradient information to explore the posterior distribution efficiently, particularly in high-dimensional parameter spaces. This method fits our model, where the posterior distribution may exhibit complex geometry due to the mixture of regimes and regime transitions.

Table 4: Transition probabilities of corn and phosphorus fertilizer prices

	Corn & P fertilizer (p_{ij})	
	Moderate (t)	High (t)
Moderate ($t+1$)	0.735	0.264
	(0.003)	(0.003)
High ($t+1$)	0.265	0.736
	(0.003)	(0.003)

Notes: Regime values of corn and phosphorus fertilizer prices, P^Y and P^F, for the moderate and high regimes, are the average values of the regime estimated from the Markov-switching Vector Autoregressive model results. Specifically, the moderate regime average prices for corn and phosphorus fertilizer are $P^Y_{\text{Moderate}} = \$1.432$, $P^Y_{\text{High}} = \$2.027$ per bu. and $P^F_{\text{Moderate}} = \$180.530$, $P^F_{\text{High}} = \$193.775$ per tn.

The likelihood of the model is constructed conditional on the latent state sequence, and prior distributions are placed on the model parameters, including the autoregressive coefficients, intercepts, and covariance matrices. Specifically, we use the priors on the intercept $\boldsymbol{\mu}_{(r_{t+1})} \sim \mathcal{N}(\mu_\mu, \sigma^2_\mu)$, priors on the autoregressive coefficients $\boldsymbol{\Phi}_{(r_{t+1})} \sim \mathcal{N}(\mu_\Phi, \sigma^2_\Phi)$, and priors on the covariance matrix $\boldsymbol{\Sigma} \sim \text{Wishart}(I, \nu)$, where I is the identity matrix and ν is the degree of freedom.[4]

MSVAR results are presented in Tables 3 and 4. The results in Table 3 show that in both regimes, the next-year corn price is significantly influenced by both the current corn price and the current P fertilizer price, as indicated by the significant coefficients for $\ln(P^Y_t)$ and $\ln(P^F_t)$. However, the next year's P fertilizer price is only influenced by its own current price, with no significant effect from the current corn price.

The asymmetry in price dynamics can be attributed to the differing market structures and roles of corn and P fertilizer. Corn, as a staple commodity, is more sensitive to input costs such as fertilizer, which directly affects production costs and, consequently, market prices. In both regimes, the significant effect of P fertilizer prices on future corn prices reflects the pass-through of input cost changes to agricultural output prices. On the other hand, the P fertilizer market is largely

[4]The mean (μ_μ, μ_Φ) and variance (σ^2_μ, σ^2_Φ) of the prior distributions are derived from the estimation results of the Markov Switching Dynamic Regression (MSDR) model, which independently estimates the price process for the Markov-switching regimes (see Appendix).

driven by supply-side factors, such as production costs and global demand for fertilizers, rather than fluctuations in corn prices. This explains why P fertilizer prices are only influenced by their own lagged values, with no significant impact from corn prices. Table 4 shows, for example, that the corn price has a 73.5% likelihood of remaining at a moderate regime during the next period given that the process is moderate during the current period as well as a 26.5% likelihood of moving to a high regime.

3.3 Values for other model parameters

Values for the remaining model parameters not estimated above are calibrated based on the literature and expert consultation with extension colleagues, and are presented in Table 5. Parameters for legacy P dynamics are primarily taken from the deterministic dynamic model of Ekholm et al. (2005). Because we introduce stochasticity into this model, we also require value for the P dynamics carryover variance ς^2, which we set at $\varsigma^2 = 9.21$ that comes from North Carolina Tidewater region data, where the variance of legacy P stock when no fertilizer was applied. This variance reflects natural fluctuations in legacy P levels due to environmental factors such as weather and soil processes, even without fertilizer input, justifying the use of the variance in the model.

Values for soil sampling costs and precision were based on the following: Standard soil sampling typically involves collecting one soil sample per 1 hectare, costing around \$4 per acre (NCAGR 2024). This assumption follows recommendations that soil samples should be taken from areas smaller than 20 acres to ensure accuracy and representativeness of the soil's nutrient levels (USDA 09.2022). Point sampling is recommended at a spacing of 209 feet, where one composite samples are collected per acre, resulting in approximately 2.47 samples per hectare (Austin et al., 2020). Thus, point sampling provides more precise information on legacy P bioavailability but is a more expensive methodology to implement. Based on this information, we assumed that the observation error variance of point sampling (σ_p) was smaller than standard sampling ($\sigma_{ss} > \sigma_{ps}$), and the cost was 2.47 times higher than standard sampling ($c_{ps} = 2.47 \cdot c_{ss}$). The values for the observation errors are denoted in Table 5. Figure 4 displays the simulation results of legacy P accumulation (mg/dm^3) over 100 years without P fertilizer application, illustrating the range of stochastic paths.[5] The solid green line represents the deterministic path with 2% decay rate that assumes no uncertainty

[5] The results depicted in Figure 4 were generated from 10,000 simulations.

Table 5: Parameters and description

	Value	Desccription
Biological Parameters		
μ_ρ	-0.02	Average rate of growth (Myyrä et al. 2007)
ς^2	9.21	Carryover variance
γ_1	0.0032	Legacy P balance parameters (Ekholm et al. 2005)
γ_2	0.00084	
γ_3	0.000186	Legacy P surplus parameters (Iho and Laukkanen 2012, Saarela et al. 1995)
γ_4	0.003	
Economic Parameters		
c_{ss}	\$4	Standard soil sampling cost per hectare (NCAGR 2024)
c_p	\$9.88	Point soil sampling cost per hectare
β	0.9345	Discount factor with 8% discount rate (Duquette et al. 2012)
σ_{ss}	0.4	Observation error of standard soil sampling
σ_p	0.05	Observation error of point soil sampling

Notes: Soil sampling cost varies depending on the institute. This paper uses the North Carolina case (NCAGR 2024, \$4 per sample).

in legacy P dynamics. The shaded area represents the range of simulation sample paths from the 5% to 95% quantile, which becomes broader as the legacy P extends further into the future. Quantile lines for the 25% (blue dots), 50% (red dash-dots), and 75% (green dashes) show the distribution of accumulation, with the 50% quantile also indicated as the median path. The black line represents the average of all simulation results.

The stochastic trend of legacy P dynamics follows closely to the deterministic path, suggesting that the parameters used in modeling legacy P dynamics and stochasticity do not deviate significantly from the deterministic trend. This consistency indicates that our model parameters effectively capture the essential dynamics of legacy P without substantial stochastic deviations. The light blue shaded area illustrates the variability and uncertainty in legacy P levels due to stochastic factors, showing a steady decline in legacy P, showing the gradual depletion of P reserves in the soil over time.

Figure 4: Legacy phosphorus accumulation without phosphorus fertilizer application

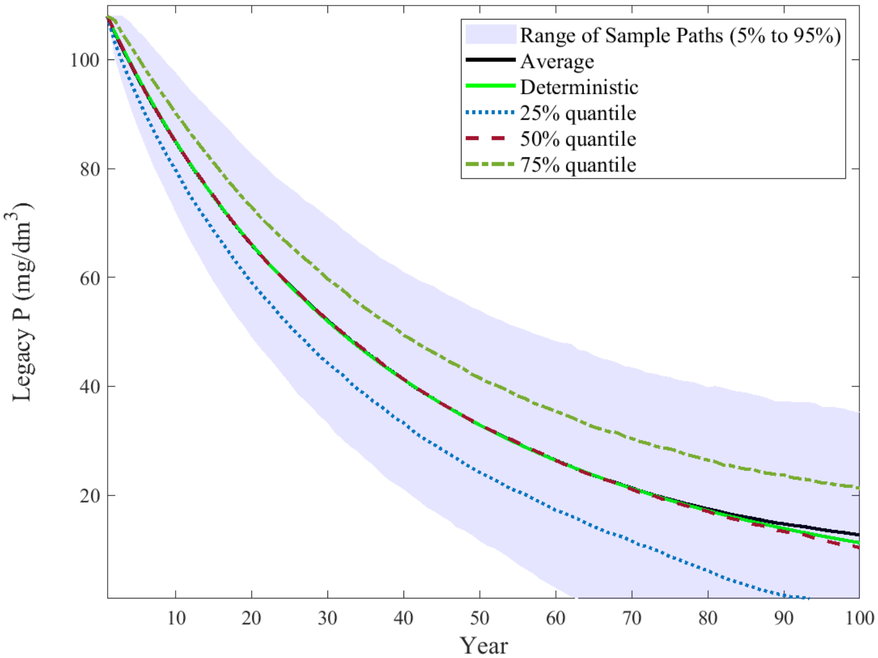

Notes: For the deterministic legacy P accumulation (green solid line), we employ a constant carry- over parameter $\rho_t = \rho = 0.98$ (2% decay rate) as adopted by Myyrä et al. (2007). The initial value is the 90th percentile (108 mg/dm^3) of legacy P in the North Carolina Tidewater data.

4 Model Results

In this section, the solution corresponding to the management model introduced in the previous sections, including state uncertainty and price stochasticity, is presented.

4.1 Optimal Policy and Dynamics of Legacy Phosphorus

Figure 5 is composed of two graphs, each illustrating the optimal policy based on the bioavailability of legacy P, uncertainty, and the economic variables of the corn and P fertilizer prices. The horizontal axis measures legacy P bioavailability (mg/dm^3) within a range of 1 to 108 mg/dm^3, which captures most of the data, reflecting the 90th percentile of legacy P levels. The vertical axis represents uncertainty, as measured by the coefficient of variation (CV) in L beleifs, from 1% to 20%.

The figure illustrates the optimal application of P fertilizer for risk-neutral farmers. When uncertainty in legacy P bioavailability is high, risk-neutral farmers tend to apply more P fertilizer

Figure 5: Optimal policy of P fertilizer application and soil sampling

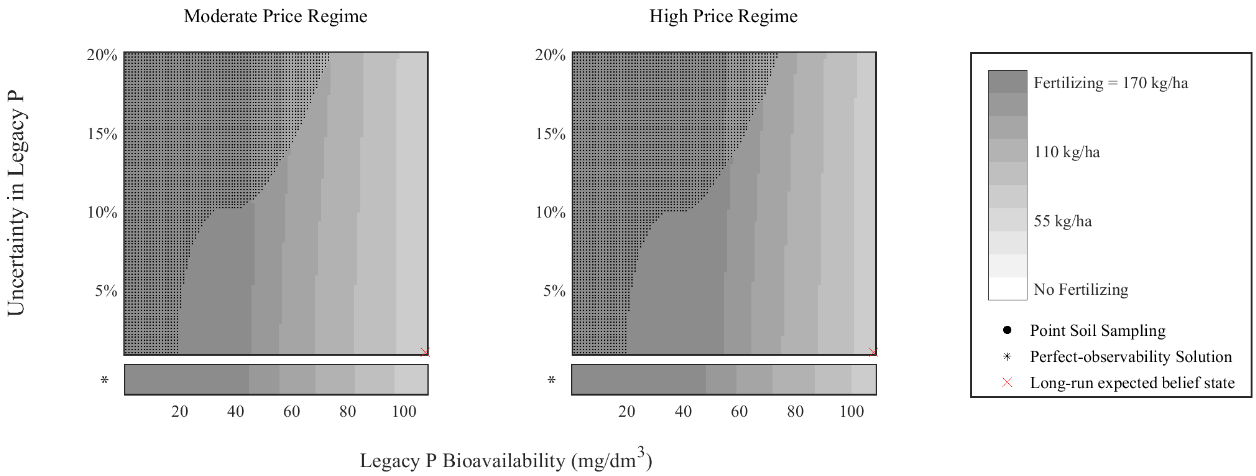

and are more likely to adopt soil sampling. The areas without dots indicate that farmers adopt standard soil sampling, while the dotted areas show where farmers opt for point sampling. When legacy P is low, farmers apply more P fertilizer to compensate for the low availability of P, ensuring sufficient nutrient supply for crop growth. Risk-neutral farmers particularly favor point sampling when legacy P level is low because it provides more accurate information, essential for making better-informed decisions about the optimal amount of P fertilizer to improve crop yield.

The perfect observability solution, marked by an asterisk, represents the scenario where farmers have perfect information about the amount of legacy P. The results for this scenario were derived using stochastic dynamic programming methods, which allow for optimal decision-making when the true state of legacy P is fully known. When the Mixed Observability Markov Decision Process (MOMDP) solution is applied in scenarios with very low uncertainty in legacy P bioavailability, the outcomes are similar to the perfect observability solution. This similarity occurs because, in cases of very low uncertainty, the farmer's belief about the legacy P state becomes highly accurate, almost equivalent to having perfect information. As a result, the decisions made under the MOMDP approach closely align with those made under perfect observability, as the need to account for uncertainty in the belief state diminishes, allowing the farmer to act almost as if they had complete knowledge of the legacy P levels.

The "×" mark represents the long-run expected belief state, where the process stabilizes over time. The position of this stable belief state is notably close to the maximum level of legacy P

Figure 6: Dynamics simulation of stochastic growth

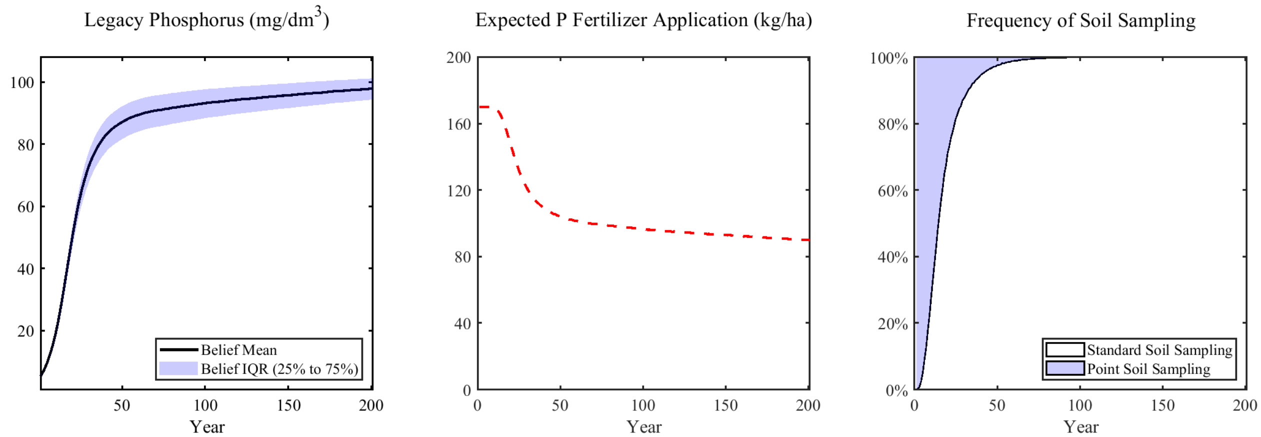

Notes: The initial values for the legacy phosphorus level and uncertainty are 5 mg/dm^3 and 10%, respectively. The initial conditions also include high corn price and high P fertilizer price. The figures were generated from simulations $i = 10,000$. The IQR for a simulation i at time t is calculated as follows:
$\text{IQR}_{it} = \left[\exp(\mu_{it}^L + \sigma_{it}^L \Phi^{-1}(0.25)), \exp(\mu_{it}^L + \sigma_{it}^L \Phi^{-1}(0.75))\right]$ where $\mu_{i,t}^L$ and $\sigma_{i,t}^L$ are the parameters of the belief state, and $\Phi^{-1}(\cdot)$ represents the inverse cumulative distribution function of the standard normal distribution (Kling et al. 2017). In Figure 6, we averaged IQR_{it} over i.

bioavailability and minimum level of uncertainty. This convergence occurs because, over time, the combination of uncertain legacy P levels and economic incentives encourages farmers to maintain or even increase legacy P through fertilization. In this scenario, farmers may be incentivized to build up legacy P reserves in response to price and uncertainty, ensuring that the resource is available for future production. As the belief system evolves, the tendency is to converge towards maximizing legacy P availability, as this offers a buffer against uncertainty and ensures higher yields when prices fluctuate. The process stabilizes when the bioavailability of legacy P reaches its maximum sustainable level, explaining why the long-term belief state aligns with the maximum legacy P level.

Additionally for the low level of uncertainty in the long-run expected belief state, as the process progresses, the information available to the farmers about legacy P becomes increasingly reliable. Over time, as farmers repeatedly observe the outcomes of their actions and adjust their practices, their belief about the amount of legacy P converges, leading to a reduction in uncertainty. This steady accumulation of knowledge and the diminishing variability in outcomes mean that farmers can predict the legacy P levels with a high degree of confidence, resulting in very low uncertainty at the steady state.

This pattern is expected to be reflected in the dynamic pattern, which further demonstrates the farmers' behavior in response to the legacy P dynamics over time. Figure 6 presents the controlled dynamics of the belief state and optimal policies over a 200-year period. The first graph in the figure shows the relationship between legacy P bioavailability over time and the uncertainty around this legacy P, depicted as the Belief IQR. The IQR visually represents the range between the 25th and 75th percentiles based on the belief states about the legacy P levels. The black line represents the mean belief, while the shaded area represents the Belief IQR.

In the early years, when farmers adopt point sampling, the uncertainty (IQR) is very low. This happens because point sampling provides detailed, precise information about legacy P levels, enabling farmers to reduce uncertainty more effectively. As a result, their beliefs about the legacy P levels are more precise, and the Belief IQR remains narrow. However, over time, as farmers shift to standard soil sampling, the uncertainty increases, causing the Belief IQR to expand. This occurs because standard sampling provides less precise information, which increases uncertainty about the exact legacy P levels in the soil. The farmers now have to rely on broader assumptions about the legacy P content, leading to a larger range in the belief about legacy P bioavailability.

The second graph shows the trend of expected P fertilizer application (kg/ha) over the periods. At the beginning of the timeline, P fertilizer application is relatively high as farmers to ensure sufficient nutrient availability for their crops. As the legacy P levels stabilize (as shown in the first graph), the need for high P fertilizer application diminishes, and farmers apply less fertilizer over time. The decreasing trend in fertilizer application indicates that farmers are relying more on the accumulated legacy P, as well as the more precise information gathered from early soil sampling, to optimize their P application.

The third graph shows the frequency of soil sampling over time, illustrating the shift from point soil sampling to standard soil sampling. Early on, when farmers are uncertain about the initial legacy P levels, they rely heavily on point sampling to gather detailed information. Over time, as legacy P stabilizes and uncertainty reduces, they shift to standard soil sampling, which is less resource-intensive but provides less precise data. This switch, as seen in the first graph, coincides with the expansion of the Belief IQR, as standard sampling contributes to greater uncertainty about legacy P.

Table 6: Estimated value of risk aversion and elasticity of intertemporal substitution in literature

Literature		RA (η)	EIS (ψ)
Howitt et al. (2005)	California (US)	1.4	0.1
Lybbert and McPeak (2012)	Chalbi (Keyna)	0.5 (OLS) 0.8 (IV)	0.7(OLS) 0.9(IV)
	Dukana (Keyna)	13.5 (OLS) 12.5 (IV)	2.8(OLS) 3.3(IV)
Augeraud-Véron et al. (2019)		0.5-11	0.1-2
Cai and Lontzek (2019)		10	0.5, 1.5
Daniel et al. (2019)		1.1-15	0.6-1.2

Notes: OLS and IV indicate Ordinary Least Squares regression and Instrumental variables estimation, respectively.

4.2 Risk Analysis: Epstein-Zin Preference

Dynamic programming mapping is an efficient method for solving belief × price MDP by breaking the optimization problem down into a sequence of subproblems. However, it assumes a risk-neutral decision-maker. To understand the effects of risk preferences on the legacy P management problem, we extended our MOMDP model by incorporating an Epstein-Zin preferences (Epstein and Zin 1989).

Since we have no data on farmer risk preference over time in this context that would have permitted on estimation of η and ψ, we chose the range of estimated parameters from the literature on environmental and agricultural studies listed in Table 6. What is more important for our analysis than specific values is the effect of high or low RA and EIS on model results. In the literature, the RA and EIS ranges are defined as $0.5 \leq \eta \leq 15$ and $0.1 \leq \psi \leq 3.3$, respectively. For our benchmark parameters, we choose multiple parameters across the ranges from which $\eta = (0.5, 15)$ and $\psi = (1.5, 3)$ were selected. In addition to benchmark parameters, the risk-neutral condition, $\eta = 0$, and the perfectly elastic intertemporal substitution, $\psi = \infty$, are considered. When $\eta = 0$ and $\psi = \infty$, the problem is reduced to the risk-neutral dynamic programming problem seeking to maximize the expected utilities.

Figure 7 represents the results of Epstein-Zin preference in MOMDP. Risk aversion (η) reflects

Figure 7: Epstein-Zin preferences and Optimal policy of P fertilizer application and soil sampling

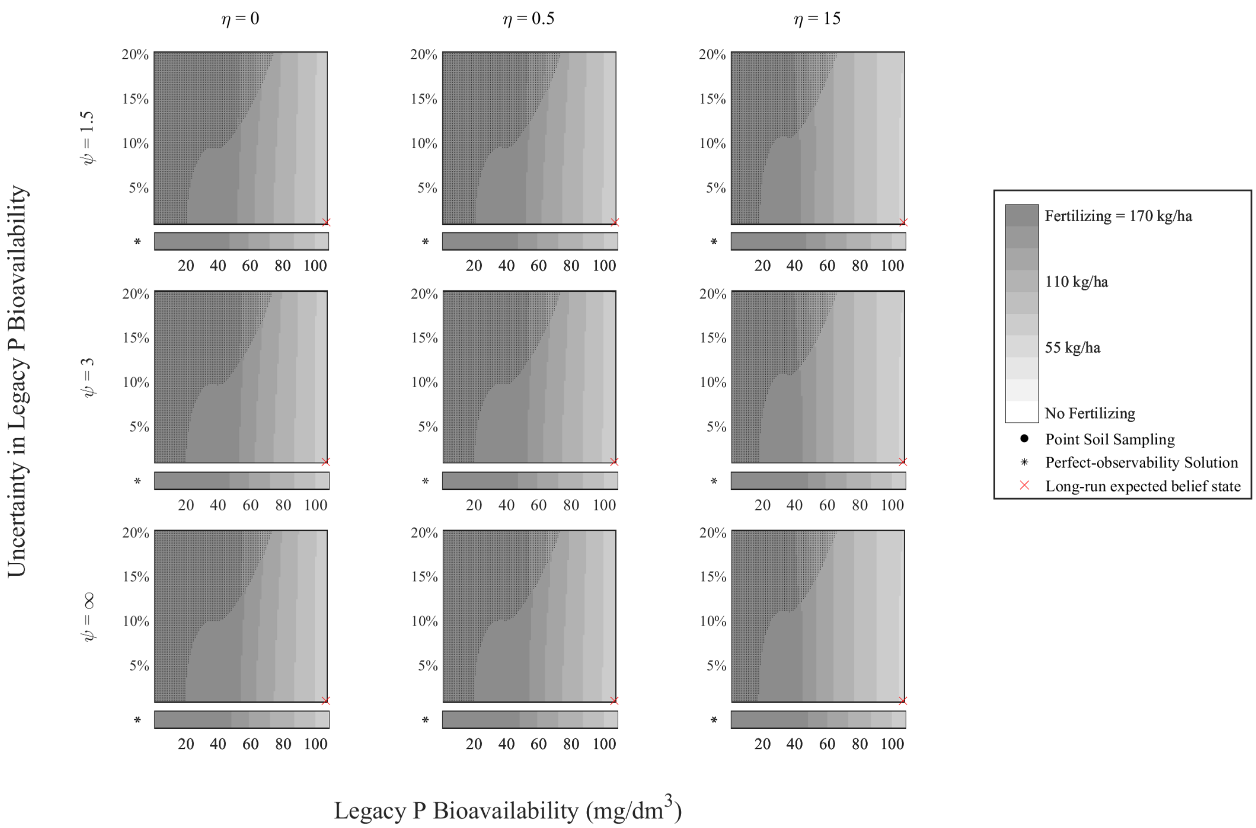

Notes: Initial price regime is high. Other initial condition results are provided in the Appendix.

farmers' attitudes toward uncertainty and potential losses. As η increases from 0 to 15, the panels demonstrate that farmers apply less P fertilizer. In the first column ($\eta = 0$), which represents a risk-neutral scenario, farmers apply more fertilizer in areas with low legacy P bioavailability. This behavior reflects a willingness to invest heavily in fertilizer to maximize yields, without concern for future risks.

However, as we move to higher levels of risk aversion $\eta = 15$, the shaded regions representing high fertilizer application shrink, particularly in areas where legacy P is more abundant. This is because risk-averse farmers are more cautious in their decision-making. They are concerned about potential future losses from over-fertilizing when future economic conditions, such as crop prices or the actual benefits of the applied fertilizer, are uncertain. In regions of high legacy P bioavailability, farmers with higher risk aversion apply less fertilizer since they prefer to rely on the existing P in the soil, reducing the risk of wasted input costs.

The vertical axis of the figure represents different values of the EIS (ψ). This parameter captures how willing farmers are to substitute consumption (or input use, like P fertilizer) between different time periods. A higher ψ value implies that farmers prefer a smoother consumption or input pattern over time, while lower values indicate that they are more willing to adjust input use based on current and future conditions. As ψ increases, the panels show that farmers become slightly more responsive to P fertilizer application, however, there is not much significant change in optimal controls.

5 Economic Sensitivity Analysis

A sensitivity analysis of economic conditions is also important for evaluating short-term productivity along with long-term agricultural sustainability when optimizing legacy P management using MOMDP. To understand the impact of varying economic conditions, we show the responses of the optimal policy to changes in the discount rate and exogenous shifts in P fertilizer price and soil sampling cost.

5.1 Discount Rate

In economic studies, particularly within agricultural and resource economics, the discount rate is a critical factor influencing farmers' decision-making processes. The discount rate essentially determines how much a farmer values future benefits compared to immediate gains. In addition to our benchmark discount rate of 8%, Duquette et al. (2012) also revealed that farmers often have relatively high discount rates, with some groups exhibiting rates as high as 43%, particularly among late adopters of new technologies, and others showing an average of 28%, especially among early adopters of best management practices. These rates are significantly higher than those typically used in benefit-cost analyses for federal programs.

In our sensitivity analysis, we selected three discount rates—8%, 28%, and 43%—to reflect a range of scenarios that align with both economic theory and empirical findings. The 28% discount rate corresponds to the average rate found among early adopters of new agricultural practices in the study by Duquette et al. (2012), representing a middle-ground scenario where future benefits are still considered, but to a lesser extent. The 43% discount rate reflects the higher end of discount rates observed among farmers, particularly those who prioritize immediate returns over future gains.

Figure 8: Sensitivity analysis: Discount rate

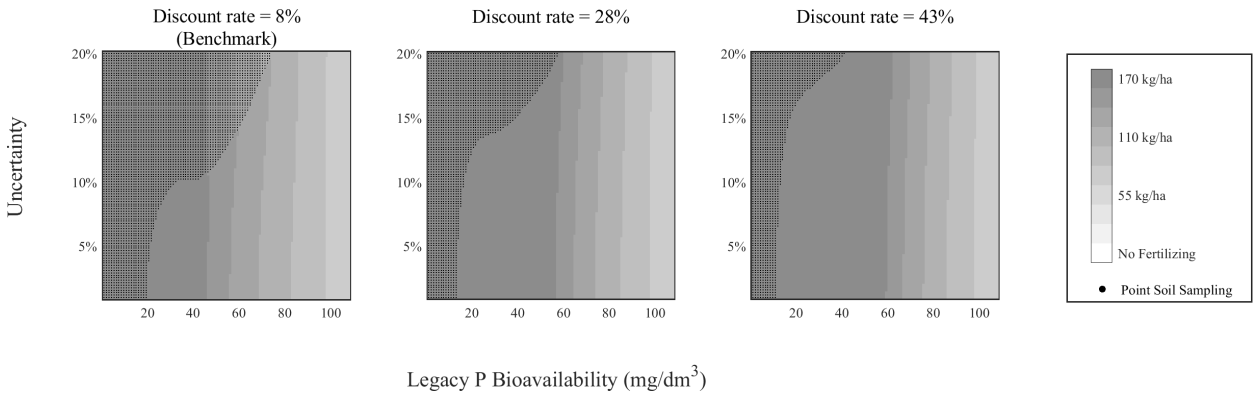

Figure 8 illustrates how varying discount rates affect farmers' decisions regarding P fertilizer application and soil sampling. At the benchmark discount rate of 8%, farmers place greater value on future benefits, leading them to adopt point sampling more frequently and apply less P fertilizer, focusing on long-term profitability. As the discount rate increases to 28% and 43%, farmers increasingly favor immediate profits, resulting in reduced point sampling and more aggressive P fertilizer application. This shift is particularly pronounced at the 43% discount rate, where the emphasis is heavily on maximizing short-term yields at the expense of long-term soil management.

The behavior observed can be explained by two economic perspectives. First, the option value of information, the benefits of acquiring precise soil data through sampling before applying fertilizer becomes more significant at lower discount rates. Farmers with a lower discount rate are more likely to invest in point sampling because they value the future flexibility and benefits that this information provides. Second, this behavior aligns with the concept of precautionary saving. By investing in point sampling, farmers improve their understanding of legacy P levels, thereby reducing the risk of future yield losses due to nutrient mismanagement. This strategic investment in information capital is more likely to occur when farmers place greater importance on future outcomes, as seen with lower discount rates.

5.2 Taxation on Phosphorus Fertilizer

Taxation on fertilizers to restrict chemical fertilization is a method to prevent water damage and this tool is incorporated by many states into their own environmental policies (Osteen and Kuchler 1986,

Figure 9: Sensitivity analysis: taxation on phosphorus fertilizer

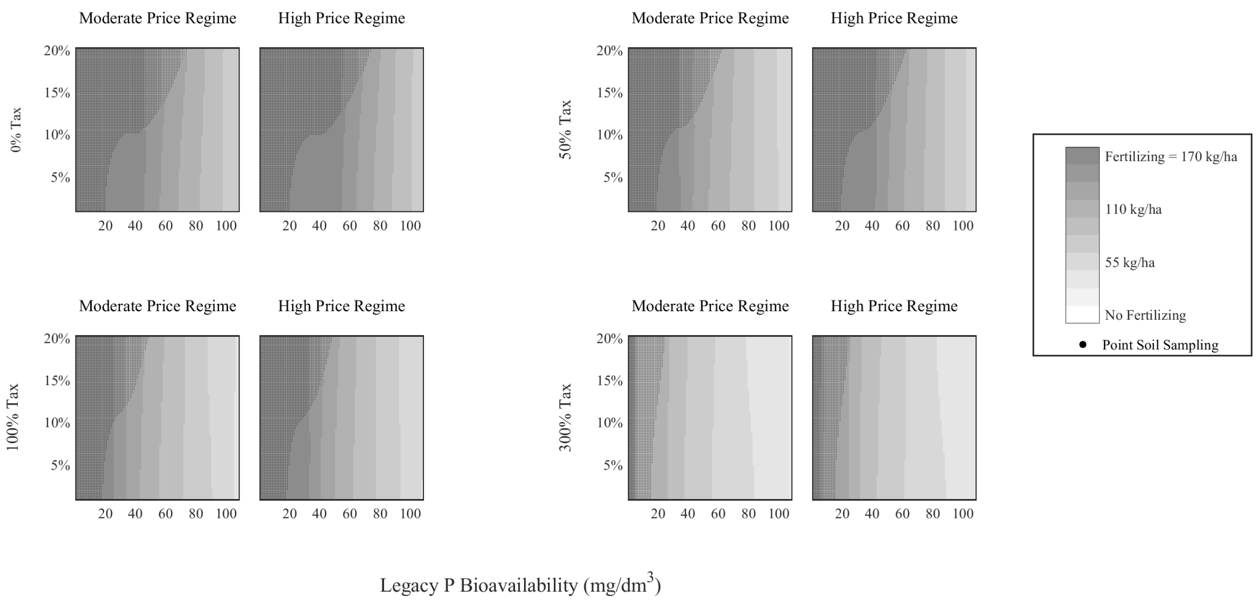

Notes: x-axis and y-axis indicate legacy P bioavailability and uncertainty in legacy P bioavailability, respectively.

Liang et al. 1998). However, the effectiveness of taxation on agricultural chemicals in reducing chemical fertilization is unclear. Liang et al. (1998) examined the effect of taxation on P and nitrogen on fertilizer use through two tax schemes, namly uniform and differentiated taxes. Their study revealed that a 500% tax reduced only 8% of on-farm fertilizer usage but caused at least a 30% reduction in agricultural labor.

This section recounts our investigation of possible explanations for fertilizer demand with legacy P state uncertainty. For the general sensitivity analysis, a uniform tax scheme is considered with tax rates of up to 0%, 50%, 100%, and 300%. The uniform tax scheme can be defined as follows: $P^F_{\text{tax}} = P^F \cdot (1 + \textit{Tax Rate})$, where P^F is the producer price, and P^F_{tax} denotes the price of P fertilizer paid by farmers. Figure 9 represents how increased fiscal pressure on P fertilizer prices influences fertilizer application decisions within each taxation scenario. As taxation on P fertilizer intensified, farmers become more conservative and reduce P fertilizer application.

Figure 10 illustrates that as tax rates on P fertilizer rise, risk neutral ($\eta = 0$) farmers proportionally reduce their use of P fertilizer. The reduction in P fertilizer application with high taxation reflects farmers' prioritization of immediate cost implications over long-term yield assurance. Under high taxation of P fertilizer, farmers not only reduce their P fertilizer application but also adjust

Figure 10: Risk neutral farmer responses to P fertilizer tax

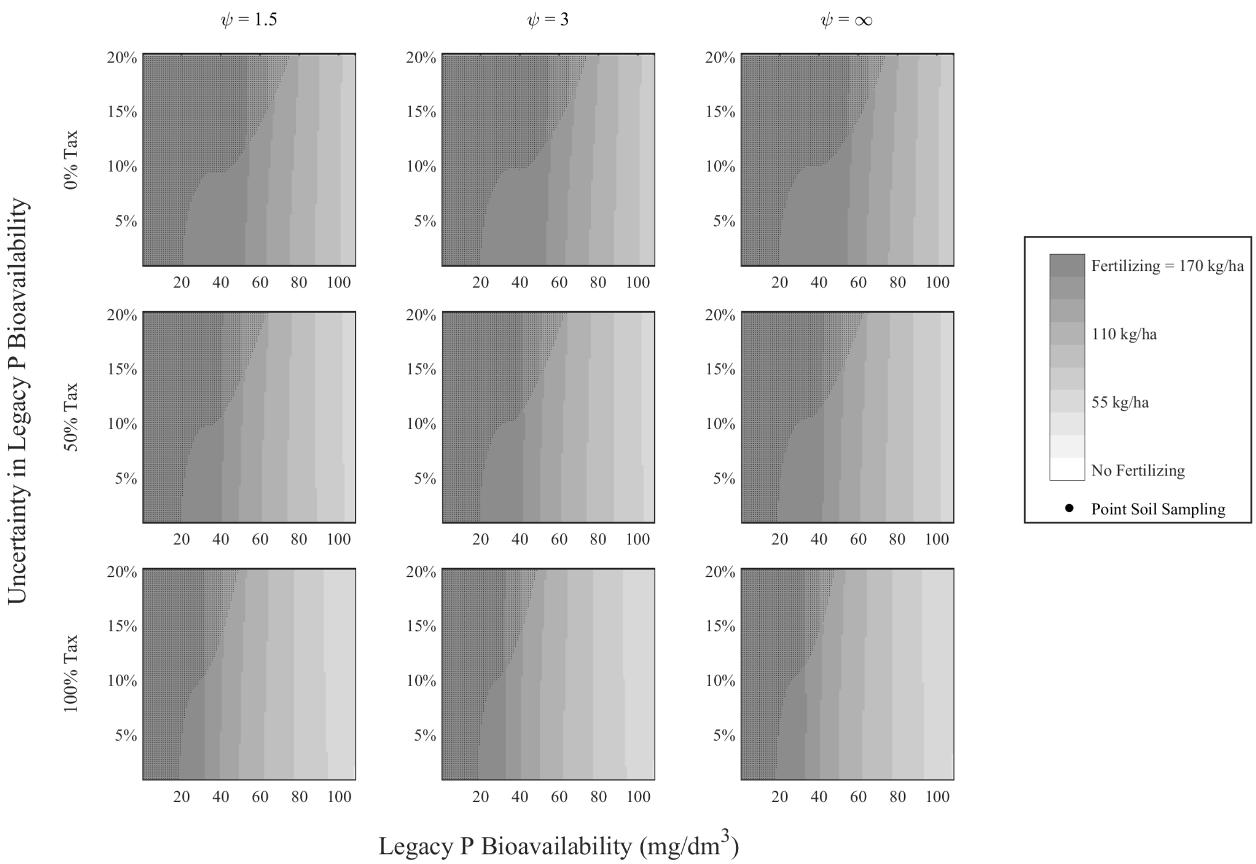

Notes: Initial price regime is high. Other initial condition results are provided in the Appendix.

their soil sampling strategies. As seen in the Figures, the increasing tax rates significantly reduce the use of point soil sampling, particularly in areas where uncertainty of legacy P bioavailability is high. This reduction in sampling occurs because high taxes make heavy fertilizer use economically burdensome, so the need for precise, costly soil sampling decreases as well.

When farmers face higher taxes, the incentive to precisely monitor soil nutrient levels diminishes because the financial burden of fertilizer application outweighs the benefits of fine-tuned soil management. In other words, as the cost of applying fertilizer rises, the payoff from optimizing fertilizer use through detailed soil sampling declines. Farmers shift toward a more conservative approach, applying less fertilizer overall and thus requiring less frequent or precise soil sampling. This behavior reflects a broader strategy to reduce costs—by cutting both fertilizer application and the associated costs of soil sampling—since the immediate economic returns from optimizing fertilizer use are diminished under high taxation.

5.3 Subsidy on Soil Sampling

The adoption of soil sampling subsidies is a forward-looking agricultural policy instrument aimed at improving nutrient management practice among farmers. We study the potential impact of various levels of uniform subsidies on soil sampling rate, $c_s^{\text{subsidy}} = c_s(1 - \textit{Subsidy Rate})$, at 0%, 30%, 60% and full (100%) subsidization. The results presented in Figure 11 reflect a clear trend: As the subsidy rate increased, a corresponding rise occurs in the adoption of point sampling, particularly with full subsidy.

This propensity toward greater point sampling is indicative of a growing awareness and appreciation among farmers for the role of precise legacy P data in sustainable management. With subsidies easing financial loads, farmers are more inclined to assess the fertility of their soil, thus gaining valuable information that can inform their economic decisions. The increase in point sampling, driven by subsidies, offers significant potential for long-term shifts in P management practices. As farmers become increasingly informed with detailed data derived on soil sampling, we may observe a refinement in P fertilizer application strategies, tailored to the precise needs of crops.

Figure 12 illustrates the impact of soil sampling subsidies on farmers with $\psi = \infty$, mapped against RA levels as denoted by $\eta = (0, 0.5, 15)$. The analysis shows that as η increased, farmers tend to apply P fertilizer at lower rates, regardless of the subsidy levels for soil sampling. While financial incentives can encourage the adoption of point sampling. This suggests that although subsidies make point sampling more accessible, the ingrained risk aversion and the perceived need to ensure crop yield stability drive continued high P fertilizer application rates. The results indicate that subsidies can effectively promote point sampling, but that their influence on reducing fertilizer application is moderated by a farmer's risk preferences.

The findings presented in Figures 11 and 12 have important implications for policy design. Policy makers should consider structuring subsidy programs to not only reduce the cost of soil sampling but also address the underlying risk preferences of farmers. Combining financial incentives with risk management education and tools can enhance the overall effectiveness of such programs. Providing farmers with education and resources to better understand and manage risks associated with nutrient management can complement subsidy programs. By reducing the perceived risks

Figure 11: Sensitivity analysis: subsidy on soil sampling

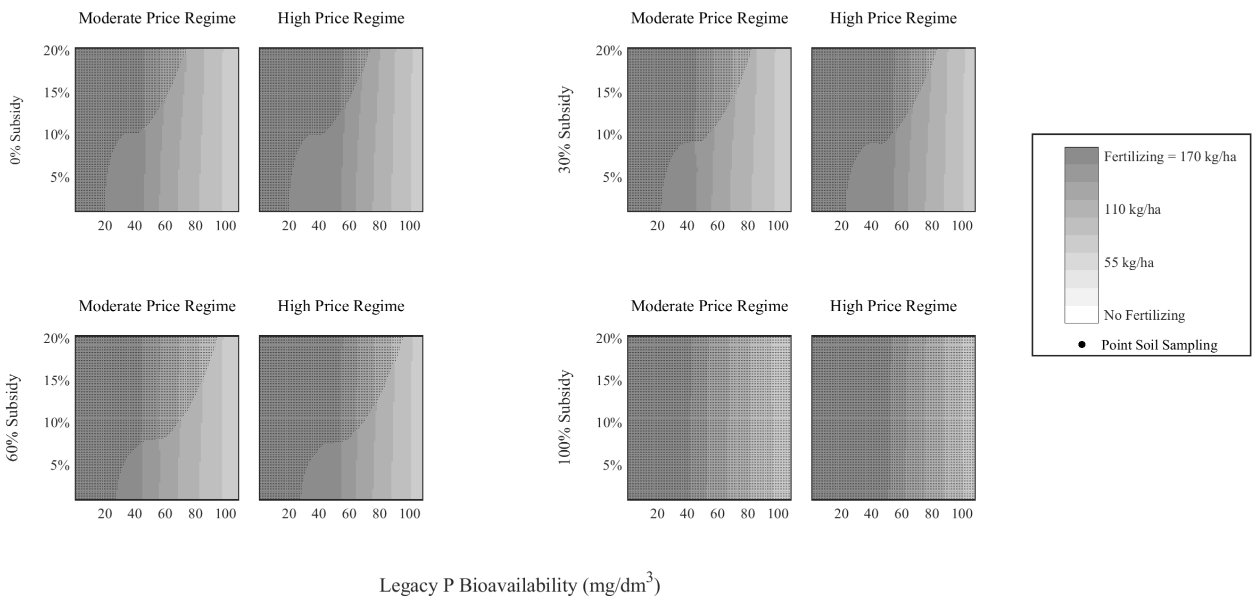

Notes: x-axis and y-axis indicate legacy P bioavailability and uncertainty in legacy P bioavailability, respectively.

related to crop yields, farmers may be more inclined to adjust their fertilizer application strategies.

Overall, while subsidies play a significant role in promoting soil sampling, addressing risk aversion through complementary measures is essential for achieving substantial change in fertilizer application practices. This comprehensive approach needs to be explored as a future project and can support sustainable P management, ensuring both agricultural productivity and environmental protection

6 Discussion

The overuse of P fertilizer in agriculture causes significant surface water pollution, necessitating policy solutions that encourage farmers to use less P fertilizer while minimizing economic losses in agricultural production. Because of the dynamic and stochastic nature of P accumulation in soil, combined with state uncertainty about legacy P stocks, this research adopts a model-based approach to disentangling these dynamics and their effects on the fertilizer demand and soil sampling behaviors of risk-averse farmers. We apply methods developed for the resource management problems involving the partial observability of resource stocks and advance these methods to

Figure 12: Risk-averse farmer responses to soil sampling subsidy

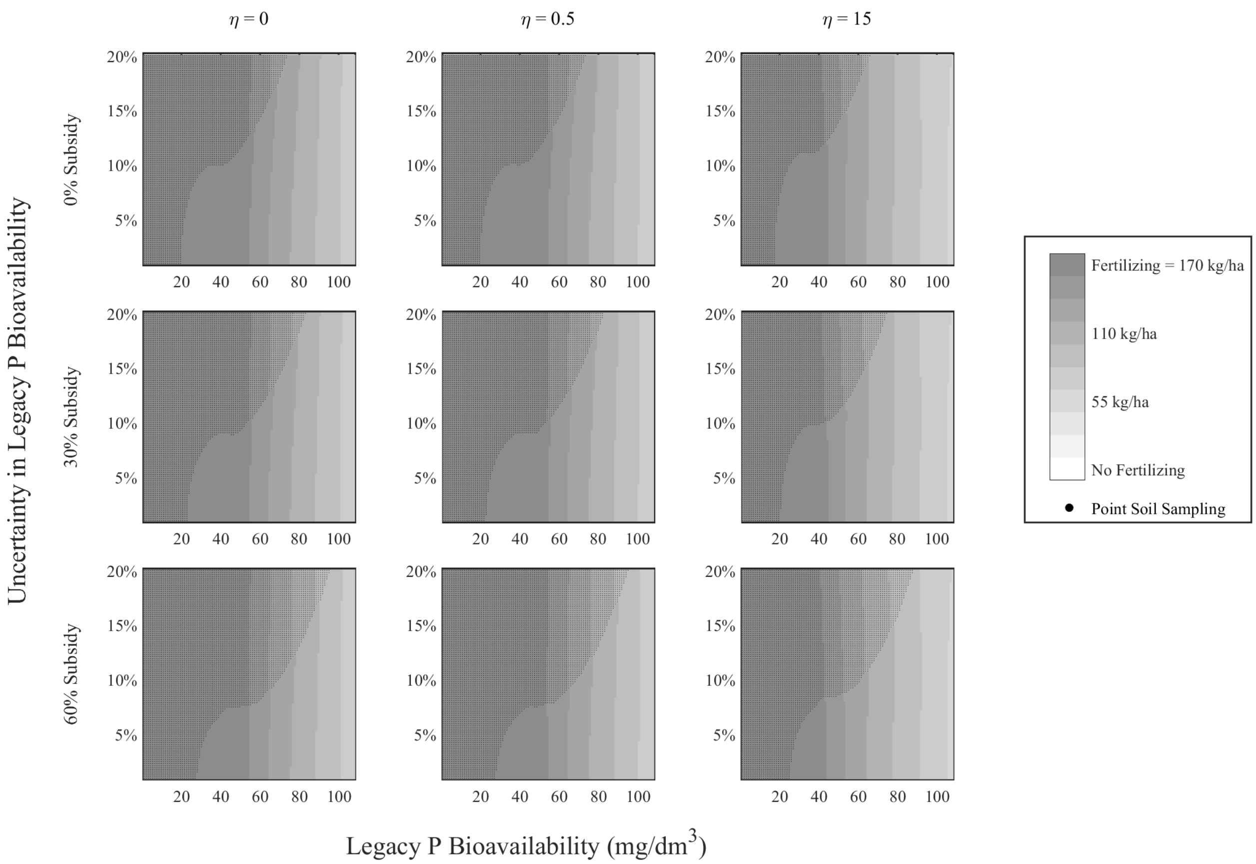

Notes: Initial price regime is high. Other initial condition results are provided in the Appendix.

include agent risk and intertemporal smoothing preferences through the Epstein-Zin preferences. Accordingly, we reveal that risk aversion among farmers significantly contributes to the demand for fertilizer and their reluctance to rely on estimated legacy P stocks, despite extensive efforts to promote the utilization of these resources.

The focus of this research is understanding behavioral change among farmers rather than the environmental damage caused by P runoff. This distinction is critical because our primary objective is to analyze how farmers respond to different economic and informational incentives concerning legacy P management. Our findings provide important insights into why farmers may not fully exploit legacy P stocks and how their risk aversion shapes their P fertilizer application decisions.

While the environmental impacts of P runoff, such as eutrophication and GHG emissions, are important, our study specifically targets farmer behavior. By understanding the decision-making processes of farmers, we can better design policies that are more likely to be adopted and effectively reduce the overconsumption of P fertilizer. Behavioral focus advances the creation of more practical and applicable solutions tailored to the needs and preferences of farmers, ultimately leading to more sustainable agricultural practice. This focus on farmer behavior can be extended in future research to incorporate environmental factors more explicitly. For instance, expanding the model to consider the environmental and climate change implications of P management can provide a more comprehensive grasp of the overall impact of agricultural practices. Future studies can integrate spatial variability and explore interactions between farmland and adjacent areas, thus offering deeper insight into the collective economic and environmental outcomes of P fertilizer and soil sampling decisions.

Future research can also consider the multiple agents involved in the optimal management of the legacy P problem with additional areas. Currently, the environmental and resource economics literature using POMDP or MOMDP generally explores single agents in their models. Some researchers examine multiple agents, but they construct separate problems for each agent and disregard the interaction between the control exercised by each agent and the unobservable state problem. However, in a collective study of legacy P management, there will be multiple agents, in addition to farmers, that have their own observations and beliefs about the environmental state, which may also include beliefs about other agents' actions and strategies. By incorporating inter-agent dynamics into our POMDP model (Emery-Montemerlo et al. 2004), the POMDP may be constructed and extended as a 'Partially Observable Stochastic Game' (POSG) to solve for the optimal policy among multiple, competitive, or cooperative, agents' profits (Hansen et al. 2004).

This study demonstrates the significant influence of risk aversion on farmer behavior, highlighting the need for policies that only provide economic incentives but also address the underlying risk preferences of farmers. Our research centers on farmer related aspects of decision-making regarding P fertilizer application and soil sampling, laying the groundwork for future explorations that integrate environmental impacts and multi-agent dynamics, farmer associated factors, and government initiatives, offering an exhaustive approach to sustainable agricultural practices.

References

ARROW, K., P. DASGUPTA, L. GOULDER, G. DAILY, P. EHRLICH, G. HEAL, S. LEVIN, K.-G. MÄLER, S. SCHNEIDER, D. STARRETT, AND B. WALKER (2018): "Are we consuming too much?" *Journal of Economic Perspectives*, 11(1), 17.

AUGERAUD-VéRON, E., G. FABBRI, AND K. SCHUBERT (2019): "The value of biodiversity as an insurance device," *American Journal of Agricultural Econoics*, 101(4), 1068–1081.

AUSTIN, R., L. GATIBONI, AND J. HAVLIN (2020): "Soil sampling strategies for site-specific field management," *NC State Extension AG-439-36*.

CAI, Y. AND T. S. LONTZEK (2019): "The social cost of carbon with economic and climate risks," *Journal of Political Economy*, 127(6), 2684–2734.

CHADèS, I., T. G. MARTIN, S. NICOL, M. A. BURGMAN, H. P. POSSINGHAM, AND Y. M. BUCKLEY (2011): "General rules for managing and surveying networks of pests, diseases, and endangered species," *Proceedings of the National Academy of Sciences*, 108(20), 8323–8328.

CHEN, L. (2022): "Essays on the Economics of Soil Health Practices," *North Carolina State University*.

CLARK, C. W. (2010): "General rules for managing and surveying networks of pests, diseases, and endangered species," *Mathematical Bioeconomics: The Mathematics of Conservation. Wiley*.

CONLEY, D. J., H. W. PAERL, R. W. HOWARTH, D. F. BOESCH, S. P. SEITZINGER, K. E. HAVENS, C. LANCELOT, AND G. E. LIKENS (2009): "Controlling eutrophication: Nitrogen and phosphorus," *Science*, 323(5917), 1014–1015.

DANIEL, K. D., R. B. LITTERMAN, AND G. WAGNER (2019): "Declining CO2 price paths," *Proceedings of the National Academy of Sciences*, 116(42), 20886–20891.

DENBALY, M. AND H. VROOMEN (1993): "Dynamic fertilizer nutrient demands for corn: A cointegrated and error-correcting system. American Journal of Agricultural Economics," *American Journal of Agricultural Economics*, 75(1), 203–209.

DOWNING, J. A., S. POLASKY, S. M. OLMSTEAD, AND S. C. NEWBOLD (2021): "Protecting local water quality has global benefits," *Nature Communications*, 12(1), 2709.

DUQUETTE, E., N. HIGGINS, AND J. HOROWITZ (2012): "Farmer discount rates: Experimental evidence," *American Journal of Agricultural Economics*, 94(2), 451–456.

EKHOLM, P., E. TURTOLA, J. GRÖNROOS, P. SEURI, AND K. YLIVAINIO (2005): "Phosphorus loss from different farming systems estimated from soil surface phosphorus balance," *Agriculture, Ecosystems and Environment*, 110(3-4), 266–278.

EMERY-MONTEMERLO, R., G. GORDON, J. SCHNEIDER, AND S. THRUN (2004): "Approximate solutions for partially observable stochastic games with common payoffs," *Proceedings of the Third International Joint Conference on Autonomous Agents and Multiagent Systems*.

EPSTEIN, L. G. AND ZIN (1991): "Substitution, risk aversion, and the temporal behavior of consumption and asset returns: An empirical analysis," *Journal of Political Economy*, 99(2), 261–286.

EPSTEIN, L. G. AND S. E. ZIN (1989): "Substitution, risk aversion, and the temporal behavior of consumption and asset returns: A theoretical framework," *Econometrica*, 57(4), 937.

FACKLER, P. AND K. PACIFICI (2014): "Addressing structural and observational uncertainty in resource management," *Journal of Environmental Management*, 133, 27–36.

FACKLER, P. L. (2014): "Structural and observational uncertainty in environmental and natural resource management," *International Review of Environmental and Resource Economics*, 7(2), 109–139.

FAN, X., M. I. GèMEZ, S. S. ATALLAH, AND J. M. CONRAD (2020): "A Bayesian state-space approach for invasive species management: the case of spotted wing drosophila," *American Journal of Agricultural Economics*, 102(4), 1227–1244.

FEDERAL RESERVE BANK OF MINNEAPOLIS (2024.04): "Consumer Price Index, 1913-," *https://www.minneapolisfed.org/about-us/monetary-policy/inflation-calculator/consumer-price-index-1913-*.

GATIBONI, L., D. OSMOND, AND D. HARDY (2022): "Changes in the Phosphorus Fertilizer Recommendations for Corn, Soybean, and Small Grains in North Carolina," *NC State Extension AG-439-30*.

GILBERT, R. J. (1979): "Optimal depletion of an uncertain stock," *The Review of Economic Studies*, 46(1), 47.

GOETZ, R. U. AND D. ZILBERMAN (2000): "The dynamics of spatial pollution: The case of phosphorus runoff from agricultural land," *Journal of Economic Dynamics and Control*, 24(1), 143–163.

HAIGHT, R. G. AND S. POLASKY (2010): "Optimal control of an invasive species with imperfect information about the level of infestation," *Resource and Energy Economics*, 32(4), 519–533.

HAMILTON, J. D. (1989): "A new approach to the economic analysis of nonstationary time series and the business cycle," *Econometrica*, 57(2), 357.

HANSEN, E. A., D. S. BERNSTEIN, AND S. ZILBERSTEIN (2004): "Dynamic Programming for Partially Observable Stochastic Games," *American Association for Artificial Intelligence.*

HOWITT, R. E., S. MSANGI, A. REYNAUD, AND K. C. KNAPP (2005): "Estimating intertemporal preferences for Natural Resource Allocation," *American Journal of Agricultural Economics*, 87(4), 969–983.

IHO, A. AND M. LAUKKANEN (2012): "Precision phosphorus management and agricultural phosphorus loading," *Ecological Economics*, 77, 91–102.

INNES, R. (2000): "The economics of Livestock Waste and its regulation," *American Journal of Agricultural Economics*, 82(1), 97–117.

KLING, D. M., J. N. SANCHIRICO, AND P. L. FACKLER (2017): "Optimal Monitoring and control under state uncertainty: Application to lionfish management," *Journal of Environmental Economics and Management*, 84, 223–245.

Kovacs, D. L., W. Li, N. Fukuta, and T. Watanabe (2012): “Mixed Observability Markov decision processes for overall network performance optimization in Wireless Sensor Networks,” *2012 IEEE 26th International Conference on Advanced Information Networking and Applications*.

Lake Erie LaMP (2011): “Lake Erie Binational Nutrient Management Strategy: Protecting Lake Erie by Managing Phosphorus,” *Prepared by the Lake Erie LaMP Work Group Nutrient Management Task Group*.

Liang, C. L. K., S. B. Lovejoy, and J. G. Lee (1998): “”Green Taxes”: Impacts On National Income, Social Welfare, And Environmental Quality,” *Working Paper*.

Livingston, M., M. J. Roberts, and Y. Zhang (2015): “Optimal sequential plantings of corn and soybeans under price uncertainty,” *American Journal of Agricultural Economics*, 97(3), 855–878.

Lötjönen, S., E. Temmes, and M. Ollikainen (2020): “Dairy farm management when nutrient runoff and climate emissions count,” *American Journal of Agricultural Economics*, 102(3), 960–981.

Loury, G. C. (1978): “The optimal exploitation of an unknown reserve,” *The Review of Economic Studies*, 45(3), 621–638.

Lybbert, T. J. and J. McPeak (2012): “Risk and intertemporal substitution: Livestock portfolios and off-take among Kenyan pastoralists,” *Journal of Development Economics*, 97(2), 415–426.

MacLachlan, M. J., M. R. Springborn, and P. L. Fackler (2017): “Learning about a moving target in resource management: optimal Bayesian disease control,” *Journal of Environmental Economics and Management*, 99(1), 140–161.

Melbourne, B. A. and A. Hastings (2008): “Extinction risk depends strongly on factors contributing to stochasticity,” *Nature*, 454(7200), 100–103.

Morales, N. A., L. Gatiboni, D. Osmond, R. Vann, S. Kulesza, C. Crozier, and D. Hardy (2023): “Critical soil test values of phosphorus and potassium for soybean and corn in three long-term trials in North Carolina,” *Soil Science Society of America Journal*, 87(2), 278–290.

Myyrä, S., K. Pietola, and M. Yli-Halla (2007): “Exploring long-term land improvements under land tenure insecurity,” *Agricultural Systems*, 92(1-3), 63–75.

NCAGR (2024): “Agronomic Services - Soil Testing: Tests and Fees- Homeowners.” *North Carolina Department of Agricultura & Consumer Service, Retrieved from https://www.ncagr.gov/divisions/agronomic-services/soil-testing/homeowners/tests-and-fees*, accessed October 11, 2024.

Osmundsen, K. K., T. S. Kleppe, and A. Oglend (2021): “MCMC for Markov-switching models—Gibbs sampling vs. marginalized likelihood,” *Communications in Statistics-Simulation and Computation*, 50(3), 669–690.

Osteen, C. and F. Kuchler (1986): “Potential Bans of Corn and Soybean Pesticides: Economic Implications for Farmers and Consumers. AER-546,” *Economics Research Service*, U.S.Department of Agriculture.

Paudel, J. and C. L. Crago (2020): “Environmental externalities from agriculture: Evidence from water quality in the United States,” *American Journal of Agricultural Economics*, 103(1), 185–210.

Rabotyagov, S. S., C. L. Kling, P. W. Gassman, N. N. Rabalais, , and R. E. Turner (2014): "The economics of dead zones: Causes, impacts, policy challenges, and a model of the Gulf of Mexico hypoxic zone," *Review of Environmental Economics and Policy*, 8, 58–79.

Ringeval, B., J. Demay, D. S. Goll, X. He, Y. P. Wang, E. Hou, ..., and S. Pellerin (2018): "A global dataset on phosphorus in agricultural soils. Scientific Data," *Scientific Data*, 11(1), 17.

Rout, T. M., J. L. Moore, and M. A. McCarthy (2014): "Prevent, search or destroy? A partially observable model for invasive species management," *Journal of Applied Ecology*, 51(3), 804–813.

Saarela, I., A. Järvi, H. Hakkola, and K. Rinne (1995): "Field Trials on Fertilization 1977-1994." *Agrifood Research Finland Bulletin*, 16.

Sattari, S. Z., A. F. Bouwman, K. E. Giller, and M. K. van Ittersum (2012): "Residual soil phosphorus as the missing piece in the global phosphorus crisis puzzle," *Proceedings of the National Academy of Sciences*, 109(16), 6348–6353.

Schnitkey, G. D. and M. J. Miranda (1993): "The Impact of Pollution Controls on Livestock-Crop Producers," *Journal of Agricultural and Resource Economics*, 18(1), 25–36.

Sims, C., D. Finnoff, A. Hastings, and J. Hochard (2017): "Listing and delisting thresholds under the Endangered Species Act," *American Journal of Agricultural Economics*, 99(3), 549–570.

Sloggy, M. R., D. M. Kling, and A. J. Plantinga (2020): "Measure twice, cut once: Optimal Inventory and harvest under volume uncertainty and Stochastic Price Dynamics," *Journal of Environmental Economics and Management*, 103, 102357.

Springborn, M. and J. N. Sanchirico (2013): "A density projection approach for non-trivial information dynamics: Adaptive management of stochastic natural resources," *Journal of Environmental Economics and Management*, 66(3), 609–624.

Tomberlin, D. and T. Ish (2007): "When is logging road erosion worth monitoring. In Proceedings of the International Mountain Logging and 13th Pacific Northwest Skyline Symposium (pp. 239-244)," *Oregon State University, College of Forestry Corvallis Oregon*.

US EPA (1995): "In National Nutrient Assessment Workshop: Proceedings, December 4-6," *United States Environmental Protection Agency, Washington, D.C.*

USDA (09.2022): "Small Scale Solutions for Your Farm - Soil Testing," *U.S. Department of Agriculture-Natural Resource and Convservation Service*.

USDA (2020): "Legacy Phosphorus Project," *United States Department of Agriculture*.

USDA (2024a): "Fertilizer Use and Price," *United States Department of Agriculture*, https://www.ers.usda.gov/data-products/fertilizer-use-and-price/.

——— (2024b): "U.S. Bioenergy Statistics," *United States Department of Agriculture*, https://www.ers.usda.gov/data-products/u-s-bioenergy-statistics/.

White, B. (2005): "An economic analysis of Ecological Monitoring," *Ecological Modelling*, 189(3-4), 241–250.

WIRONEN, M. B., E. M. BENNETT, AND J. D. ERICKSON (2018): "Phosphorus flows and legacy accumulation in an animal-dominated agricultural region from 1925 to 2012," *Global Environmental Change*, 50, 88–99.

ZHOU, E., M. C. FU, AND S. I. MARCUS (2010): "Solving continuous-state POMDPs via density projection," *IEEE Transactions on Automatic Control*, 55(5), 1101–1116.

ZOU, T., X. ZHANG, AND E. A. DAVIDSON (2022): "Global trends of cropland phosphorus use and sustainability challenges," *Nature*, 611(7934), 81–87.

Appendix

Evaluating Optimal Farm Management of Phosphorus Fertilizer Inputs with Partial Observability of Legacy Soil Stocks[1]

Chanheung Cho Zachary S. Brown David M. Kling Luke Gatiboni Justin S. Baker

[1]Cho: North Carolina State University (ccho5@ncsu.edu); Brown: North Carolina State University (zsbrown2@ncsu.edu); Kling: Oregon State University (David.Kling@oregonstate.edu); Gatiboni: North Carolina State University (luke_gatiboni@ncsu.edu); Baker: North Carolina State University (jsbaker4@ncsu.edu).

A Methodology and Algorithms

This appendix offers further details and elaborates on the methodology described in paper. It begins with the foundation of partially observable Markov decision processes (POMDP) and mixed-observability Markov decision process (MOMDP), two-stage belief updating process, basis of Markow-swithcing Vector autoregressive model (MSVAR), and concludes by presenting supplementary figures.

A.1 Detailed formulation of the Dynamic Programming Model

The Bellman equation for the recursive expected utility function eq. (6) can be detailed as:

$$\begin{aligned} V(\boldsymbol{S_t}) = \max_{F,s} & \iint \pi(\boldsymbol{S_t}, F_t, s_t) f(P^Y_{t+1} \mid P^Y_t, P^F_t) b_t(L_t) dP^Y_{t+1} dL_t \\ & + \beta \iint p(P_{r_{t+1}} \mid P_{r_t}) p(O^s_{t+1} \mid b_{t+1}(L_t), s_t) V(\boldsymbol{S_{t+1}}) dO^s_{t+1} dP_{r_{t+1}}, \end{aligned} \tag{A1}$$

and given Epstein-Zin preferences, eq. (8) can be further detailed as:

$$\begin{aligned} V_{EZ}(\boldsymbol{S_t}) = \max_{F,s} \Bigg[& (1-\beta) \left(\iint \pi(\boldsymbol{S_t}, F_t, s_t)^{1-\eta} f(P^Y_{t+1} \mid P^Y_t, P^F_t) b_t(L_t) dP^Y_{t+1} dL_t \right)^{\frac{1-\psi^{-1}}{1-\eta}} \\ & + \beta \left(\iint p(P_{r_{t+1}} \mid P_{r_t}) p(O^s_{t+1} \mid b_{t+1}(L_{t+1}), s_t) V_{EZ}(\boldsymbol{S_{t+1}})^{1-\eta} dO^s_{t+1} dP_{r_{t+1}} \right)^{\frac{1-\psi^{-1}}{1-\eta}} \Bigg]^{\frac{1}{1-\psi^{-1}}}, \end{aligned} \tag{A2}$$

under state variables, $\boldsymbol{S_t} \equiv [b_t(L_t),\, P^Y_t,\, P^F_t]$ at time t and P_{r_t} is set of the corn and phosphorus (P) fertilizer prices P^Y_t and P^F_t in regime r_t at time t.

A.2 Solution Methods of Projected Belief

Continuous state POMDP has challenges due to an infinite-dimensional belief space and because approximating belief states by discretization can lead to computational issues. Exact evaluation of the posterior distribution is difficult to address, and even structuring the belief updating process in discretized space is often infeasible. To address this challenge, a density projection technique suggested by Zhou et al. (2010) and employed by Kling et al. (2017) in economics is utilized.

Density projection projects the infinite-dimensional belief space onto a low-dimensional parameterized family of densities.[2] Projection mapping from the belief state $b(L)$ to exponential family of density $f(L;\theta)$, where θ is a natural parameter, is achieved by minimizing the *Kullback-Leibler* (KL) divergence between $b(L)$ and $f(L;\theta)$ as:

$$\begin{aligned} b^P(L) &\triangleq \arg\min_f \; D_{KL}(b \parallel f) \\ &\text{where } D_{KL}(b \parallel f) \triangleq \int b(L) \log \frac{b(L)}{f(L;\theta)} dL \\ &\forall L, b(L) > 0 \leftrightarrow f(L;\theta) > 0 \end{aligned} \tag{A3}$$

and thus belief $b(L)$ and its projection $f(L;\theta)$ satisfies:

$$\mathbb{E}_b[T_j(L)] = \mathbb{E}_\theta[T_j(L)] \quad \text{for } j = 1, 2, ..., J \tag{A4}$$

where $T(L)$ is the sufficient statistics of the probability density (Zhou et al. 2010).

Bayesian updating of projected belief state is implemented adopting a particle filtering, which uses a Monte Carolo simulation approach to estimate the belief state with a limited set of particles (samples) and simulates the transition of the belief state (De Freitas 2001, Arulampalam et al. 2002). In the particle filtering, particles L_t^i for $i = 1, 2, ..., Z$ are drawn from $b_t(L_t)$ and L_{t+1}^i from the propagation $p(L_{t+1}|L_t, F_t, s_t)$. This allows for the approximation of $b_{t+1}(L_{t+1})$ by the probability mass function (Zhou et al. 2010):

$$b_{t+1}(L_{t+1}) \approx \sum_{i=1}^{Z} \tau_{t+1}^i \phi(L_{t+1} - L_{t+1}^i) \tag{A5}$$

where $\tau_{t+1}^i \propto p(O_{t+1}^l | L_{t+1}^i, F_t, s_t)$, denoting the associated weight and ϕ represent the Kronecker

[2]Technical interpretation of density projection and particle filtering hereafter closely follows Zhou et al. (2010).

delta function. Substituting equation (A5) into (A4), the approximation becomes:

$$\begin{aligned}\mathbb{E}_{b_{t+1}}[T_j(L_{t+1})] &= \int T_j(L_{t+1}) b_{t+1}(L_{t+1}) dL_{t+1} \\ &\approx \int T_j(L_{t+1}) \left[\sum_{i=1}^{Z} \tau_{t+1}^i \phi(L_{t+1} - L_{t+1}^i) \right] dL_{t+1} \\ &= \sum_{i=1}^{Z} \tau_{t+1}^i T_j(L_{t+1}^i) \\ &= \mathbb{E}_{\theta_{t+1}}[T_j(L_{t+1})]\end{aligned} \tag{A6}$$

simplified by the properties of the Kronecker delta function. Thus, if the particles L_t^i are drawn from the projected belief state $b_t^P = f(\cdot;\theta_t)$ and their propagation L_{t+1}^i satisfy the $\sum_{i=1}^{Z} \tau_{t+1}^i T_j(L_{t+1}^i) = \mathbb{E}_{\theta_{t+1}}[T_j(L_{t+1})]$, the transition probability of θ_t to θ_{t+1} can be calculated.

Density projection effectively reduces infinite-dimensional density to low-dimensional, parameter-defined density, transforming the belief Markov decision process (MDP) into a more manageable and solvable form referred to as 'projected belief MDP'. In this paper, the legacy P states are defined as the natural parameters of log-normal distribution and transform to the θ in the 'projected belief MDP' calculation (Kling et al. 2017). The utilization of the log-normal distribution in parameterized density is particularly advantageous, primarily due to its tractability to positive-valued state variables and its parametric simplicity characterized by two parameters: mean and coefficient variation (Sloggy et al. 2020).

While there are numerous ways to solve the projected belief MDP, we follow Kling et al. (2017) and discretize the projected belief MDP space into a discrete-state space. Because the value function in eq. (6) and (8) is a function both of the belief and price states, we then compute the value function on a grid of all discretized possible belief and price state combinations.

The projected belief Markov decision process (MDP) is a low-dimensional, continuous state MDP (Zhou et al. 2010). To facilitate the value iteration, we first convert the projected belief MDP into a discrete state MDP.[3] This conversion involves discretizing the space of natural parameters θ in the exponential distribution $f(\cdot|\theta)$ (Zhou et al. 2010). In this paper, we employ the log-normal distribution to define legacy P bioavailability μ_L and uncertainty in legacy P bioavailability as

[3]The discretization and estimation methods are adopted from Zhou et al. 2010 and Kling et al. 2017.

coefficient variation (ν), $\nu_L = \sigma_L/\mu_L$ with a parameter set $\delta = \{\mu_L, \nu_L\}$. Hence, we discretize θ by calculating the univariate log-normal parameters μ and σ that $\theta = \{\mu, \sigma\}$ where $\sigma > 0$ from the δ (Kling et al. 2017). The calculation of μ and σ is follows:

$$\mu = \ln\left(\frac{\mu_L^2}{\sqrt{\mu_L^2 + \sigma_L^2}}\right), \qquad \sigma^2 = \ln\left(1 + \frac{\sigma_L^2}{\mu_L^2}\right). \tag{A7}$$

For the estimation in discretized space, μ_L and σ_L are discretized into a 100×1 vector. A 100×100 mesh grid $\{\delta_i\}_{i=1}^N = G$ is then calculated, incorporating all grid points $\delta_i = \{\mu_{L,i}, \nu_{L,i}\}$ where $\nu_{L,i} = \sigma_{L,i}/\mu_{L,i}$. Within this discretized state space δ_i, the crop profit function is evaluated as the expected value of δ_i, in associated with controls F, s and prices P^Y, P^F. By defining the transition probability as $\tilde{p}(\delta_i, F, s)(\delta_j)$, representing the probability to transitioning from δ_i to δ_j, the discretized belief MDP for eq (A1) is formulated as:

$$\begin{aligned}\tilde{V}(\delta_i, P^Y, P^F) = &\max_{F,s} \tilde{\pi}(\delta_i, F, P^{Y'}, P^F, s) \\ &+ \beta \sum^{P^{F'}} \sum^{P^{Y'}} \sum_{j=1}^{N} p(P_{r'} \mid P_r)\tilde{p}(\delta_i, F, s)(\delta_j)\tilde{V}(\delta_j, P^{Y'}, P^{F'}),\end{aligned} \tag{A8}$$

where $p(P_{r'} \mid P_r)$ denote the discretized transition probability of corn price P^Y and P fertilizer price P^F, estimated from the MSVAR model.[4]

The profit function $\tilde{\pi}(\delta_i, F, P^Y, P^F, s)$ and transition probability $\tilde{p}(\delta_i, F, s)(\delta_j)$ associated with controls F and s can be estimated by using Monte-Carlo simulation, as follows (Zhou et al. 2010):

[4] In price dynamics, the $t+1$ state is represented by $'$ notation.

Algorithm 1. Estimation of Crop Profit Function

Input: $\delta_i, P^Y, P^F, F, s, \boldsymbol{\omega}^2$

Output: $\tilde{\pi}(\delta_i, F, P^Y, P^F, s)$

Step 1. Sampling:

$$\boldsymbol{L} = f^{-1}(\boldsymbol{\omega}^2|\theta_i) \qquad \text{where } \boldsymbol{L} = \{L_1, L_2, ..., L_Z\}$$

Step 2. Estimation:

$$\tilde{\pi}(\delta_i, F, P^{Y'}, P^F, s) = \frac{1}{Z}\sum_{j=1}^{Z}\sum^{P^{Y'}} \pi(L_j, F, P^{Y'}, P^F, s) f(P^{Y'} \mid P^Y, P^F)$$

Source: Zhou et al. (2010)

$\boldsymbol{\omega}^k$ is the set of Sobol points $\boldsymbol{\omega}^k = \{\boldsymbol{\omega}_1^k, \boldsymbol{\omega}_2^k, ..., \boldsymbol{\omega}_Z^k\}$ that derived from Sobol sequence. For the estimation of crop profit function and transition probability, we use the three-dimensional ($k = 3$) Sobol points $\boldsymbol{\omega}^k$ that includes Z =10,000 points. In the draw process, the Sobol draw omits an initial 1,000 points, then select every 101st point thereafter (MathWorks. 2024). We also apply a random linear scramble along with a random digit shift. In the estimation of log-likelihood function, Sobol draw is efficient methods. To achieve the same precision level of 1,000 Sobol draws in the estimation of log-likelihood function value, the estimation requires the 1,661 Haltom draws, 4,155 Modified Latin Hyper Cube Sampling draws or 9,987 pseudo-random draws (Czajkowski and Budziński 2019). With a five-dimensional Sobol draw, the desired precision level requires at least 2,100 points (Czajkowski and Budziński 2019), and we choose the number of points to 10,000 to increase the precision level.

Estimation of transition probability $\tilde{p}(\delta_i, F, s)(\delta_j)$ is in Algorithm 2. Based on the output from Algorithm 2. and the estimated transition probabilities of corn and P fertilizer price, we proceed to calculate the comprehensive of transition probabilities $p(P_{r'} \mid P_r)\tilde{p}(\delta_i, F, s)(\delta_j)$. The combination of these probabilities is achieved through the Kronecker product of probability matrices for corn and P fertilizer prices, as well as the transition probabilities $\mathbf{P}_r \otimes \tilde{\mathbf{P}}$ (Sloggy et al. 2020), where $\mathbf{P}_r$

is the probability matrix for corn and P fertilizer prices over moderate and high regimes and $\tilde{\mathbf{P}}$ is the estimated probability matrix of $\forall i, j,\ \tilde{p}(\delta_i, F, s)(\delta_j)$.

Algorithm 2. Estimation of transition probability

Input: $\delta_i, P^Y, P^F, F, s, \boldsymbol{\omega}^1, \boldsymbol{\omega}^2, \boldsymbol{\omega}^3$

Output: $\tilde{p}(\delta_i, F, s)(\delta_j)$

Step 1. Sampling:

$$\boldsymbol{L} = f^{-1}(\boldsymbol{\omega}^2|\theta_i) \quad \text{where } \boldsymbol{L} = \{L_1, L_2, ..., L_Z\}$$

Step 2. Compute $\tilde{\boldsymbol{L}}$ by propagation of $\boldsymbol{L}$ according to the dynamics of legacy P (eq. 1) using controls F and s, and carry-over parameter ρ that is generated using $\boldsymbol{\omega}^1$.

Step 3. Compute $O_1, O_2, O_3, ..., O_Z$ from $\tilde{\boldsymbol{L}} = \{\tilde{L}_1, \tilde{L}_2, \tilde{L}_3, ..., \tilde{L}_Z\}$ using equation 5 and observation error $\{\lambda_i^l\}_{i=1}^Z$ that is generated by $\boldsymbol{\omega}^3$, where s is determined by the controls ss and ps.

Step 4. For each O_k, $k = 1, 2, ..., Z$, compute the updated belief state

$$\tilde{b}_k = \sum_{i=1}^{Z} \tau_i^k \phi(L - \tilde{L}_i),$$

where ϕ is the Kronecker delta product function and

$$\tau_i^k = \frac{p(O_k \mid \tilde{L}_i, F, s)}{\sum_{i=1}^{Z} p(O_k \mid \tilde{L}_i, F, s)}$$

Step 5. For $k = 1, 2, ..., Z$ project each $\tilde{b}_k$ onto the lognormal density to find $\tilde{\theta}_k$, and compute $\hat{\delta}_k$ from $\tilde{\theta}_k$.

Step 6. For each $k = 1, 2, ..., Z$, calculate the bilinear interpolation weight for $\tilde{\delta}_k$ on G. For each $\tilde{\delta}_k$, sum the bilinear interpolation weight.

$$\tilde{p}(\delta_i, F, s)(\delta_j) = \frac{\text{sum of bilinear interpolation weights assigned to } \delta_j}{Z}$$

Source: Zhou et al. (2010), Kling et al. (2017)

B Soil Sampling and Yield-Based Information Update

In this section, we discuss the process behind the two-stage belief updating mechanism. The two-stage approach considers the dynamic nature of decision-making in agricultural practices, where information is acquired at different points in time.

The first stage of belief updating occurs when farmers conduct soil sampling before making fertilization decisions. This initial update is crucial as it provides farmers with more accurate information about the legacy P state, allowing them to make more informed fertilization choices.

The second stage of belief updating takes place after the fertilization and harvest, when farmers receive additional information through the actual corn yield. This yield data, reflecting the results of their fertilization decisions, provides a further opportunity to update their beliefs about the legacy P state. By incorporating information from both soil sampling and yield outcomes, the two-stage belief updating process captures the evolving understanding farmers have about their fields' P conditions.

B.1 Two-Stage Belief Updating Process

Figure B1 illustrates the two-stage belief updating process within a POMDP framework. In this model, the unobservable state of legacy P L_t represents the true but hidden condition of the bioavailability at time t, which evolves to a new state L_{t+1} by the next time period. Farmers, unable to directly observe this state, rely on a sequence of observations and actions to update their beliefs about the legacy P condition.

The process begins with soil sampling s_t, where farmers obtain an initial observation $O_t^{(1)}$ that provides partial information about the current state L_t. This observation is used to update their belief from b_t to $b_t^{(1)}$ within a period, forming the first stage of belief updating. Following this, farmers apply phosphorus fertilizer F_t, and the resulting corn yield Y_t offers additional information. This yield data leads to a second update of their belief, from $b_t^{(1)}$ to b_{t+1}, as they refine their understanding of the legacy P state.

The arrows in the figure indicate the flow of information between these components, showing how observations from soil sampling and yield outcomes interact with the unobservable state to update the belief state over time. In the first belief updating process, because farmers adopt soil

Figure B1: Schematic of Two-Stage Belief Updating Process

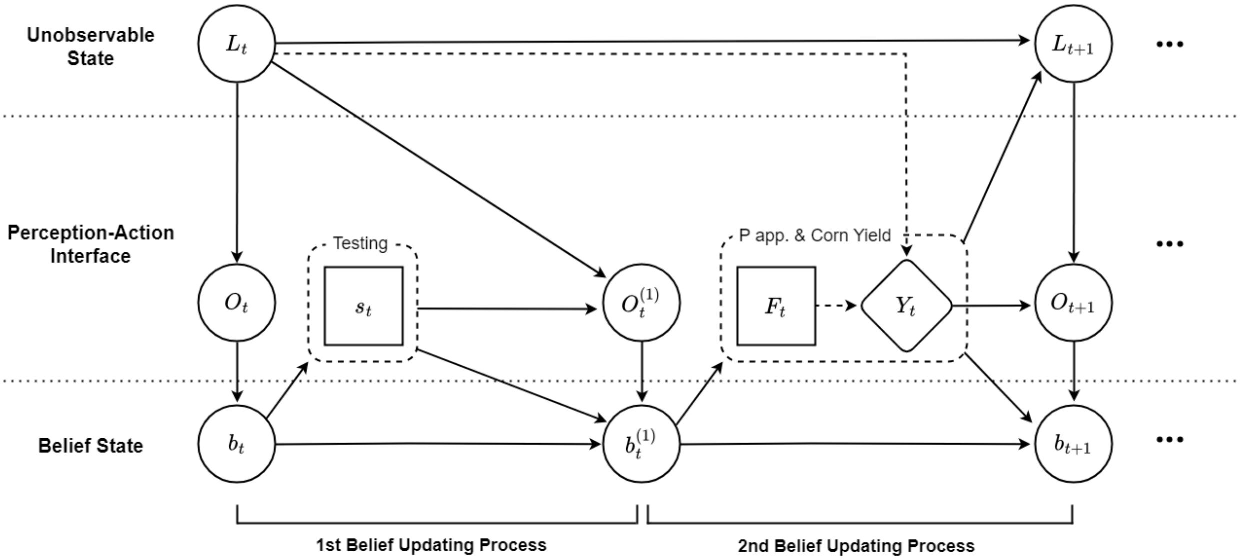

Notes: Figure A1 illustrates the two-stage belief updating process for farmers' decision-making in a POMDP framework. The first stage involves updating the belief state b_t based on soil sampling s_t, and the second stage further updates the belief using corn yield Y_t after P fertilizer application F_t.

sampling before making a P fertilizer decision, the belief updating process begins with the following equation:

$$b_t^{(1)}(L_t) \propto p(O_t^s \mid L_t, s_t) b_t(L_t), \tag{B1}$$

where O_t represents the observation obtained from soil sampling s_t. The belief $b_t(L_t)$ is updated to $b_t^{(1)}(L_t)$ based on the new information provided by the soil sampling. This updated belief reflects the farmer's revised understanding of the legacy P state L_t after considering the soil test results.

The next step in the belief updating process occurs after the corn yield Y_t is realized. The corn yield is calculated based on the current legacy P state, and it is conditional on the P fertilizer application F_t. In our model, we assume that farmers directly obtain information from the corn yield Y_t. Consequently, we assume that the observation O_{t+1} at time $t+1$ is equivalent to the yield Y_t. This assumption is based on the fact that the yield is a direct and observable outcome that strongly influences the farmer's beliefs about the soil's legacy P levels. For instance, if the yield Y_t is high, farmers are likely to believe that the soil has a high level of legacy P, suggesting that their prior application of fertilizer was effective or that the soil had sufficient nutrient reserves. Conversely, a low yield might lead farmers to adjust their beliefs toward the soil having lower legacy

P levels. By equating O_{t+1} with Y_t, we simplify the belief updating process while still capturing the essential feedback mechanism that guides farmers' future management decisions. The belief updating process at this stage is represented by the equation:

$$b_{t+1}(L_{t+1}) \propto \int p(Y_t \mid L_t, F_t) p(L_{t+1} \mid L_t, F_t) b_t^{(1)}(L_t) \, dL_t. \tag{B2}$$

Here, $b_{t+1}(L_{t+1})$ is the updated belief at time $t+1$, taking into account the information provided by the corn yield Y_t. The term $P(Y_t \mid L_t, F_t)$ represents the likelihood of observing the yield given the previous legacy P state and the fertilizer application, while $p(L_{t+1} \mid L_t, F_t)$ represents the propagation of the legacy P state from time t to $t+1$ given the fertilizer application F_t.

B.2 Defining the Corn Yield Distribution and Bayesian Updating

In this section, we define the corn yield distribution for likelihood $p(Y_t \mid L_t, F_t)$ in our Bayesian updating process. Corn yield distributions are derived from Sobol points $\boldsymbol{L}$ for each natural parameter θ_i following Algorithm 1.

These Sobol points are generated from a log-normal distribution, resulting in yield samples Y_t that align with a log-normal distribution, as shown in Figure B2. The fitted log-normal curve effectively captures this distribution, accurately representing the central tendency, variability, and skewness inherent in the yield simulations. Defining the form of the yield distribution is essential for our Bayesian updating because the yield serves as an observation in the likelihood function. By understanding the distribution of yields under varying phosphorus fertilizer applications, we can better inform the belief updating process, ensuring that our model realistically reflects the probabilistic nature of yield outcomes.

Figure B3 depicts the belief update based on information obtained from soil sampling. The prior belief distribution b_t, (shown by the red dashed line) is updated to the posterior distribution $b_t^{(1)}$, (shown by the blue solid line) after incorporating the soil sampling observation (indicated by the black dotted line). As seen in the figure, the observation provides significant information, leading to a notable shift in the belief from the prior to the posterior distribution. This substantial update indicates that the soil sampling results are effective in refining the farmer's understanding of the legacy P state, which is crucial for making informed fertilization decisions.

In contrast, Figure B4 represents the second stage of belief updating, where the belief is further adjusted based on information from the crop yield. The posterior distribution from the first stage $b_t^{(1)}$ now serves as the prior distribution in this stage, and the crop yield observation (again indicated by the black dotted line) informs the update to the final posterior distribution b_{t+1} (shown by the green solid line). However, in this stage, the crop yield provides less additional information, resulting in a less pronounced shift from the prior to the posterior distribution. The reason for this is that the crop yield, while reflective of the legacy P state, is also influenced by other factors, leading to greater uncertainty and less precise updating of the belief. Consequently, the posterior distribution has a relatively wider variation, indicating that the yield data does not significantly help the farmer's understanding of the legacy P levels compared to the soil sampling. This analysis demonstrates the critical role of soil sampling in the belief-updating process, particularly in the first stage, and in our paper, we consider soil sampling for the belief-updating process.

Figure B2: Distributions of Corn Yields

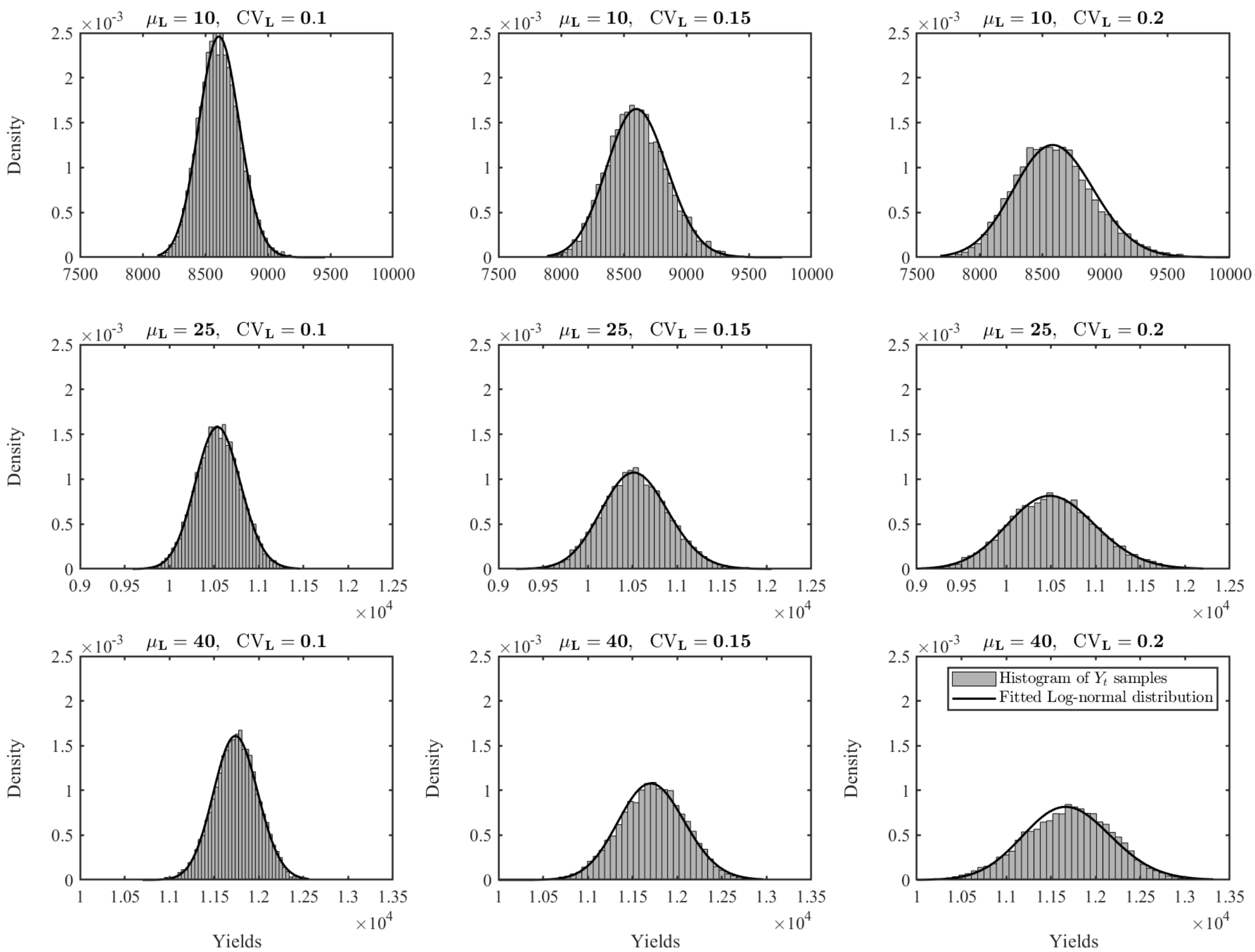

Notes: Figure B2 demonstrates that the distribution of corn yields closely follows a log-normal distribution across different mean legacy P levels (μ_L) and coefficients of variation (ν_L). The histograms of the simulated yield samples, along with the overlaid fitted log-normal curves, show a strong alignment between the empirical simulations and the log-normal distribution. This consistency across varying scenarios justifies the assumption that corn yield distributions can be appropriately modeled using a log-normal distribution in subsequent analyses.

Figure B3: First Stage Belief Updating Process

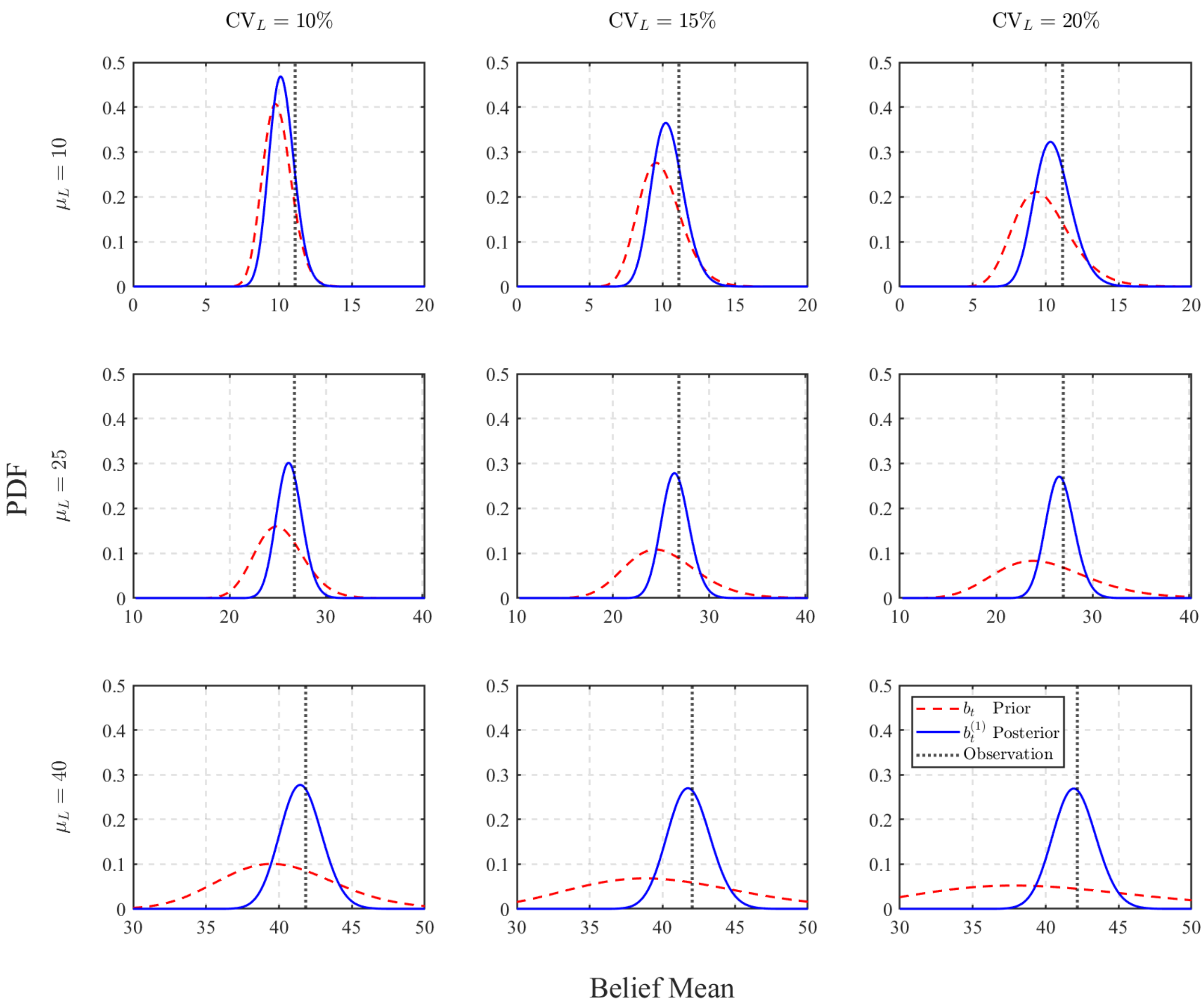

Notes: Figure B3 illustrates the prior b_t and posterior $b_t^{(1)}$ distributons across different combinations of legacy P bioavailability μ_L and uncertainty ν_L. The observation (black dotted line) is derived from soil sampling, which provides partial information about the legacy P levels. The prior belief (red dashed line) is updated to the posterior belief (blue solid line) after incorporating the soil sampling observation. Each subplot corresponds to a different combination of μ_L and ν_L, demonstrating how these parameters influence the updating process and the resulting belief distributions. As ν_L increases, the posterior distribution becomes wider, indicating greater uncertainty in the belief about the legacy P state.

Figure B4: Second Stage Belief Updating Process

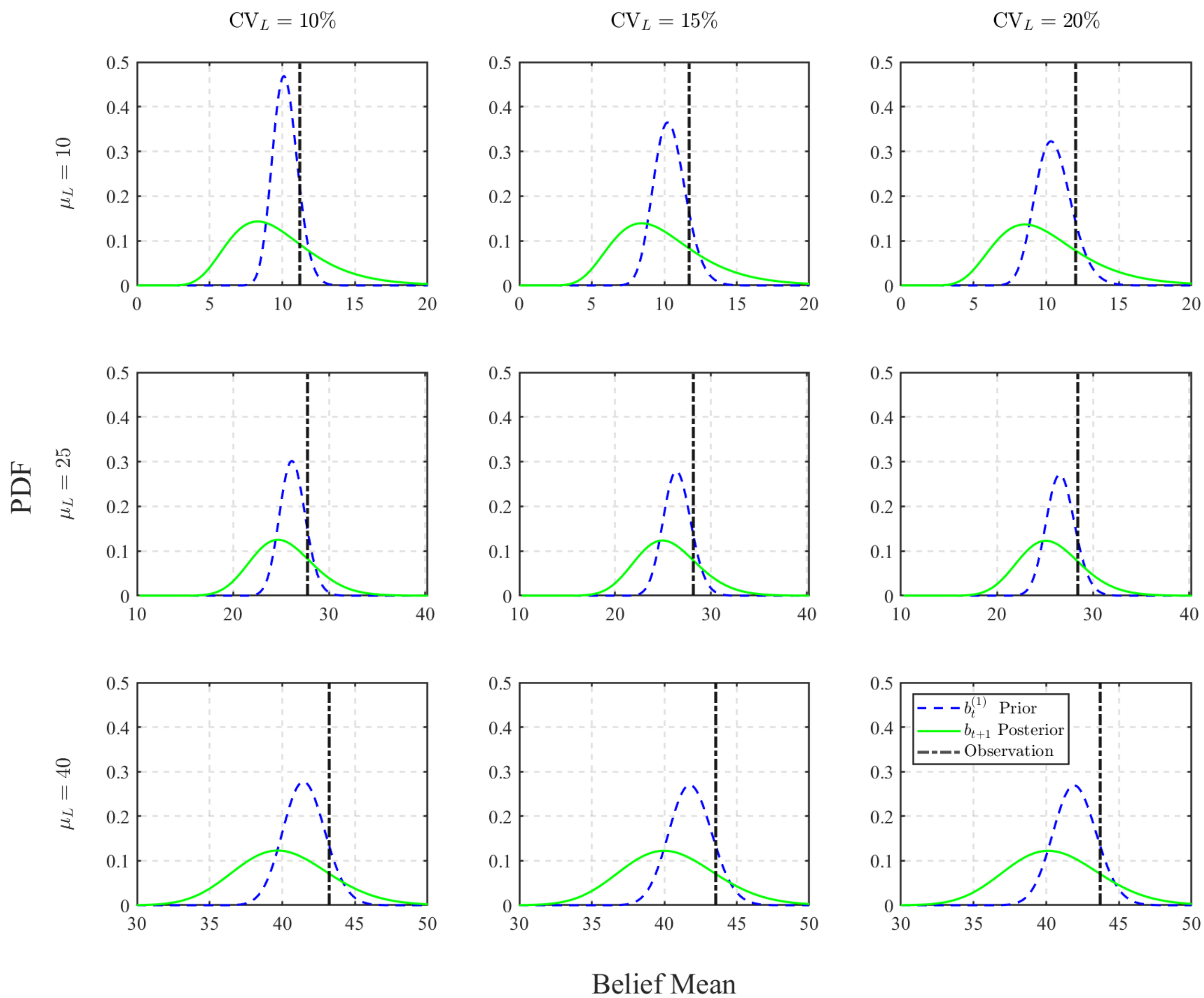

Notes: Figure B4 shows the progression from prior $b_t^{(1)}$ to posterior b_{t+1} belief distributions after incorporating additional information from the crop yield, across different combinations of legacy P bioavailability μ_L and uncertainty ν_L for the legacy P state. The observation from the crop yield is indicated by the black dashed line, which further informs the belief updating process. The prior distribution (blue dashed line) represents the belief after the first stage of updating, while the posterior distribution (green solid line) reflects the updated belief after considering the crop yield observation.

C Estimation of Price Transition: Markov-switching Dynamic Regression Model

Table C1: Markov switching dynamics regression for corn and phosphorus fertilizer prices

	Corn ($\ln(P^Y_{t+1})$)		Phosphorus fertilizer ($\ln(P^F_{t+1})$)	
	Moderate	High	Moderate	High
$\ln(P^F_t)$	0.091	0.763***	0.947***	–1.347***
	(0.186)	(0.284)	(0.151)	(0.251)
$\ln(P^Y_t)$	0.633***	0.280	–0.034	2.234***
	(0.199)	(0.205)	(0.097)	(0.470)
Const.	–0.410	–3.408**	0.275	11.866***
$(\alpha_{0,r_t}, \beta_{0,r_t})$	(0.923)	(1.448)	(0.723)	(1.862)
Std Dev.	0.109		0.075	
$(\sigma_{\epsilon,r_t}, \sigma_{v,r_t})$	(0.014)		(0.009)	
Log-likelihood	12.309		31.502	
AIC	–0.207		–1.406	

Notes: Robust standard errors are in parentheses. In the regression, constant standard deviation $\sigma^2 = \sigma_i^2 = \sigma_j^2$ is assumed for $r_t \in \{i, j\}$, $i \neq j$. *, **, and *** denote significance at the 10%, 5%, and 1% levels, respectively.

In this section, We estimate a log-linear Markow-switching Dynamic Regression (MSDR) model to construct the basis parameters of prior distributions in MSVAR model. The specification of the (MSDR) of the following form:

$$\begin{aligned} \ln(P^Y_{t+1}) &= \alpha_{0,r_{t+1}} + \alpha_{1,r_{t+1}} \ln(P^Y_t) + \alpha_{2,r_{t+1}} \ln(P^F_t) + \epsilon_{t+1} \\ \ln(P^F_{t+1}) &= \beta_{0,r_{t+1}} + \beta_{1,r_{t+1}} \ln(P^F_t) + \beta_{2,r_{t+1}} \ln(P^Y_t) + v_{t+1} \end{aligned} \tag{C1}$$

where $\alpha_{0,r_{t+1}}, \beta_{0,r_{t+1}}$ are the intercepts for price regime r_{t+1} and ϵ_{t+1}, v_{t+1} are the identical distribution (i.i.d.) normal errors with mean zero and regime-dependent variance $\sigma^2_{\epsilon,r_{t+1}}, \sigma^2_{v,r_{t+1}}$, respectively. We allow for two price regimes in the model, $r_t \in \{\text{moderate, high}\}$, based on visual inspection of the data in Figure 3.

MDSR results are presented in tables C1. To generate the basis parameters of prior distribution of intercept (μ_μ, σ^2_μ) and coefficients $(\mu_\Phi, \sigma^2_\Phi)$, we use the averaged value of estimated values (α_0, β_0) and (α_i, β_i) for each prior mean and used the averaged values of standard error to calculated the prior variances $(\sigma^2_\mu, \sigma^2_\Phi)$

D Supplementary Figures

Figure D1: Optimal policy with fixed stochasticity in growth rate

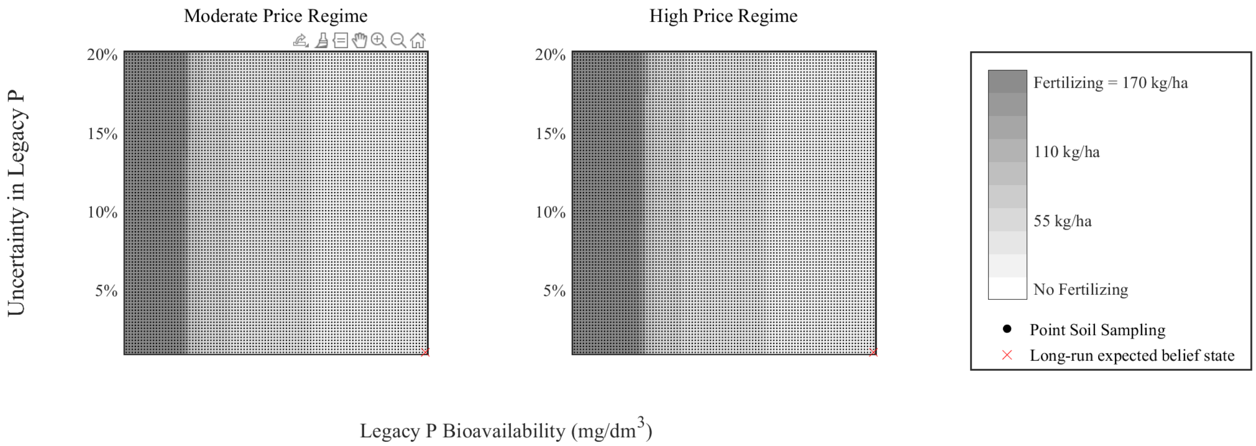

Notes: : In the original model, the standard deviation $\sigma_\rho(L)$ of the log percentage growth rate is inversely related to the legacy P level (equation 2), reflects an assumption in the model that more abundant legacy P stocks are assumed to be relatively more predictable in terms of their carry-over to the next period. Because we have no quantitative data with which to estimate the form of $\sigma_\rho(L)$, we investigate the effects of the alternative assumption that $\sigma_\rho(L) = \varsigma$ is fixed at uncertainty coefficient. This figure shows the model output derived under the alternative assumption. Given the uncertainty regardless in the dynamics scaling with legacy P levels, an optimal approach is to employ substantially more point sampling across state spaces.

Figure D2: Variance and Covariance of Residuals Across Price Regimes in MSVAR Model

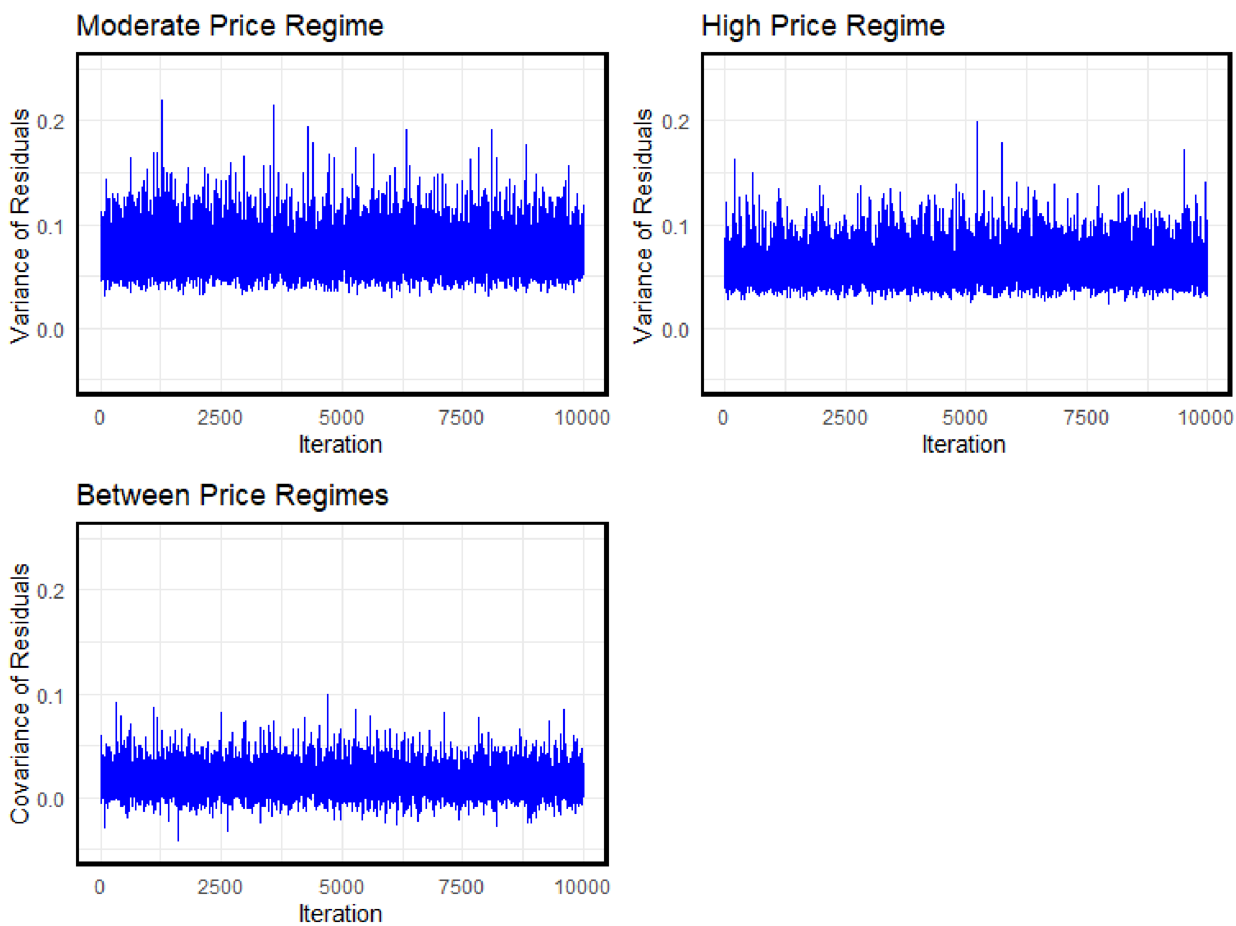

Notes: : The figure illustrates the variance and covariance of residuals for corn and phosphorus fertilizer price regimes over 10,000 iterations, based on a Markov-switching vector autoregression (MSVAR) model. The top left panel displays the variance of residuals for the moderate price regime, showing stable fluctuations. Similarly, the top right panel represents the variance of residuals for the high price regime, which follows a similar pattern of stabilization. Finally, the bottom panel shows the covariance of residuals between the moderate and high price regimes. The covariance exhibits more consistent fluctuations throughout the iterations. This figure highlights the dynamics of the model, with variances and covariances are consistent, indicating the model's convergence.

Figure D3: Risk analysis: Epstein-Zin preference (moderate price regime)

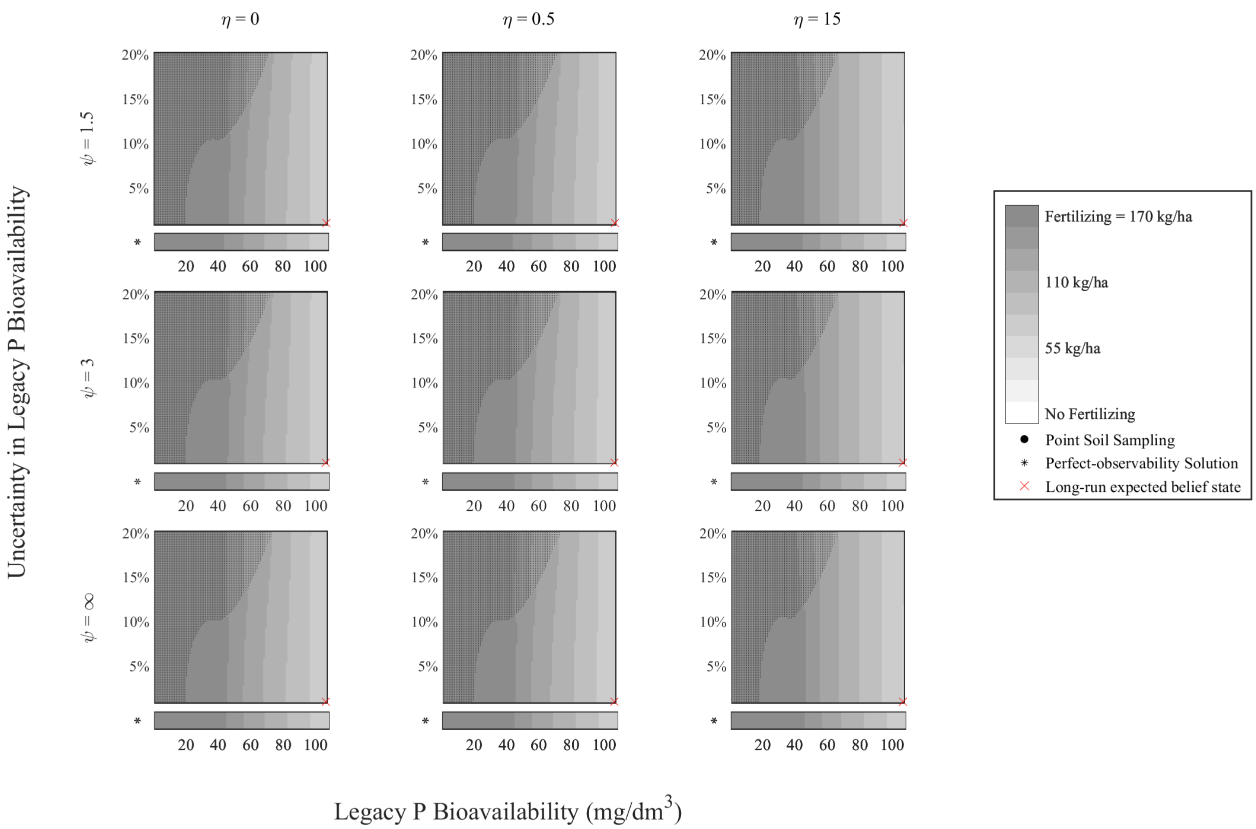

Figure D4: Risk neutral farmer responses to P fertilizer tax (moderate price regime)

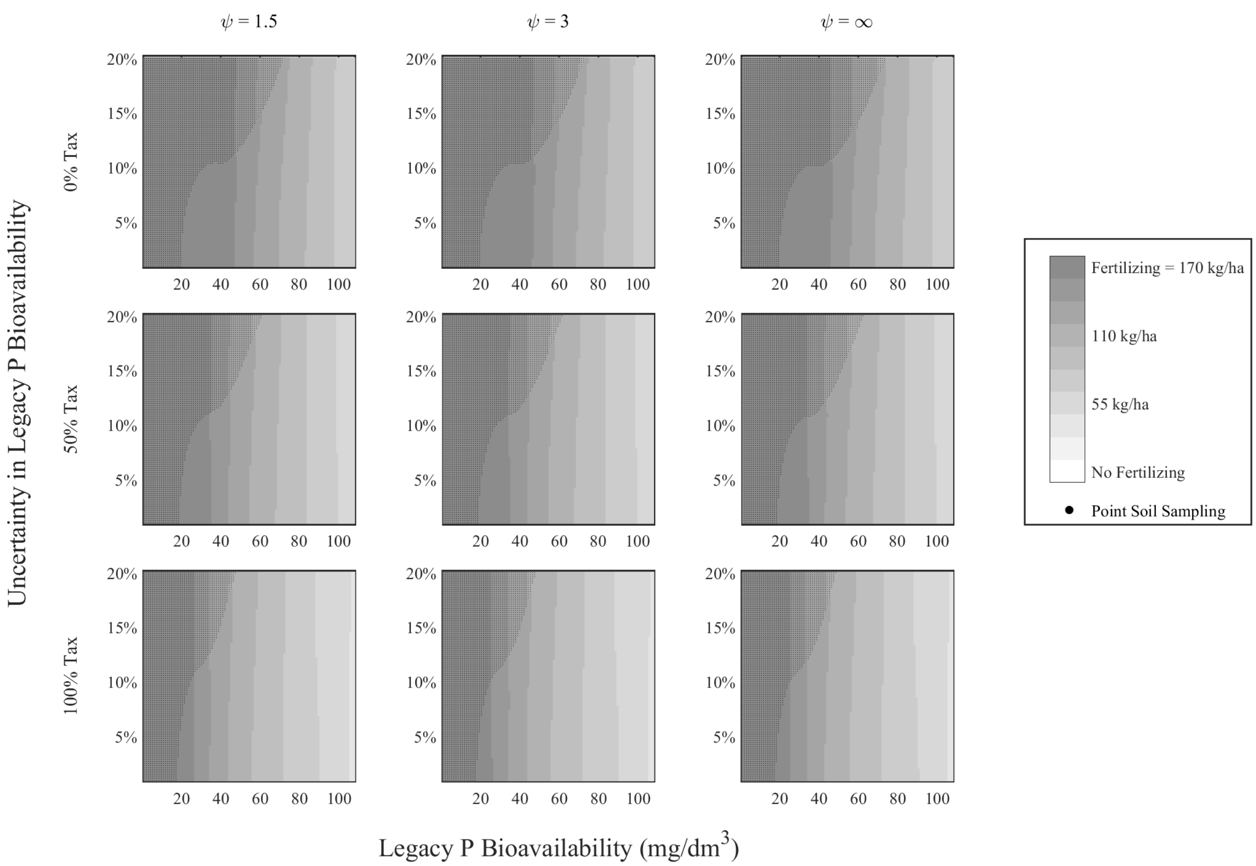

Figure D5: Risk-averse farmer responses to soil sampling subsidy (moderate price regime)

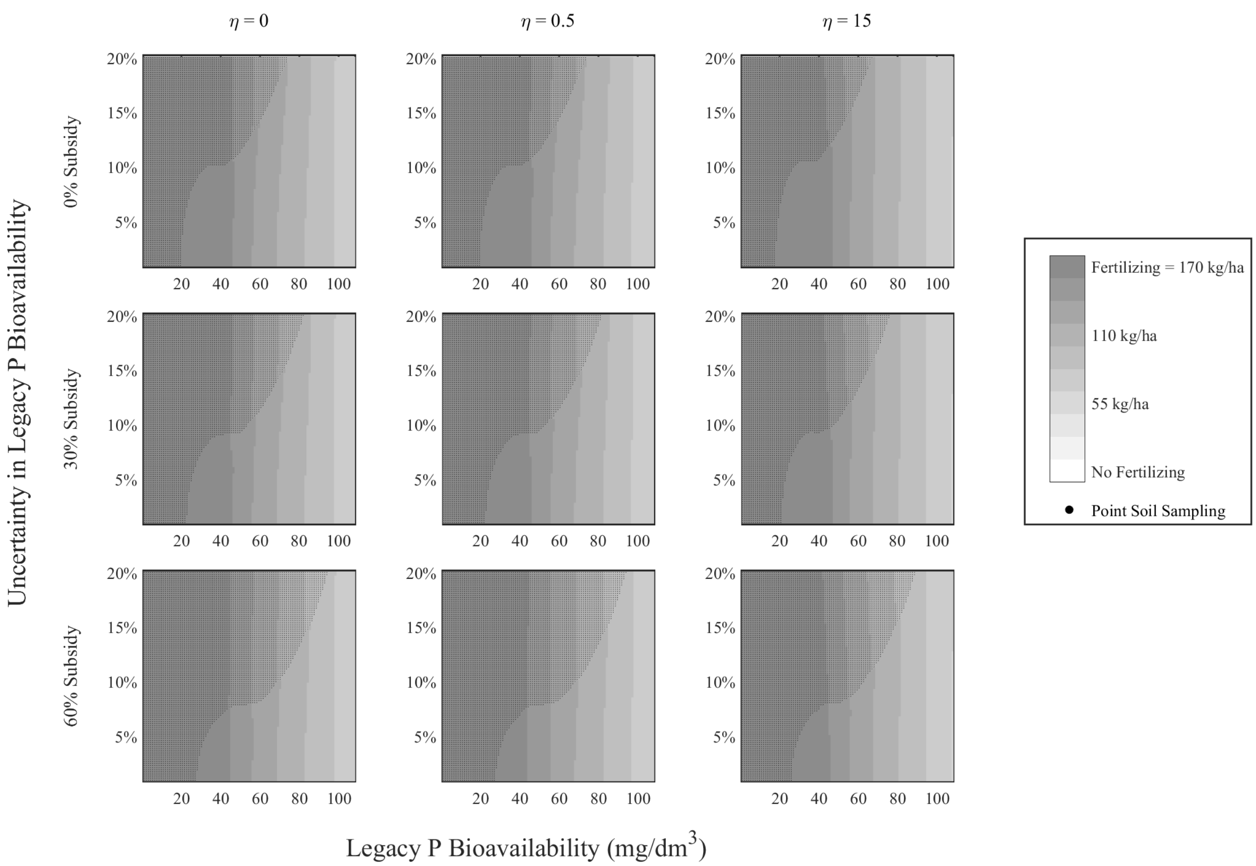

References

ARULAMPALAM, M. S., S. MASKELL, N. GORDON, AND T. CLAPP (2002): "A tutorial on particle filters for online nonlinear/non-Gaussian Bayesian tracking," *IEEE Transactions on signal processing*, 50(2), 174–188.

CZAJKOWSKI, M. AND W. BUDZIŃSKI (2019): "Simulation error in maximum likelihood estimation of discrete choice models," *Journal of Choice Modelling*, 31, 73–85.

DE FREITAS, N. (2001): "Sequential Monte Carlo methods in practice (Vol. 1, No. 2, p. 2)," *A. Doucet, & N. J. Gordon (Eds.). New York: springer*.

KLING, D. M., J. N. SANCHIRICO, AND P. L. FACKLER (2017): "Optimal Monitoring and control under state uncertainty: Application to lionfish management," *Journal of Environmental Economics and Management*, 84, 223–245.

MATHWORKS. (2024): "Sobol Sequence, MATLAB Documentation." *Retrieved from https://www.mathworks.com/help/stats/sobolset.html*, accessed September 23, 2024.

SLOGGY, M. R., D. M. KLING, AND A. J. PLANTINGA (2020): "Measure twice, cut once: Optimal Inventory and harvest under volume uncertainty and Stochastic Price Dynamics," *Journal of Environmental Economics and Management*, 103, 102357.

ZHOU, E., M. C. FU, AND S. I. MARCUS (2010): "Solving continuous-state POMDPs via density projection," *IEEE Transactions on Automatic Control*, 55(5), 1101–1116.